Los Alamos National Laboratory is operated by the University of California for the United States Department of Energy under contract W-7405-ENG-36

General-Purpose Heat Source Development: Safety Verification Test Program

Explosion Overpressure Test Series

Los Alamos
Los Alamos National Laboratory
Los Alamos, New Mexico 87545

GENERAL-PURPOSE HEAT SOURCE DEVELOPMENT: SAFETY VERIFICATION TEST PROGRAM

Explosion Overpressure Test Series

by

T. A. Cull, T. G. George, and D. Pavone

ABSTRACT

The General-Purpose Heat Source (GPHS) is a modular, radioisotope heat source that will be used in radioisotope thermoelectric generators (RTGs) to supply electric power for space missions. The first two uses will be the NASA Galileo and the ESA Ulysses missions. The RTG for these missions will contain 18 GPHS modules, each of which contains four $^{238}PuO_2$-fueled clads and generates 250 $W_{(t)}$. A series of Safety Verification Tests (SVTs) was conducted to assess the ability of the GPHS modules to contain the plutonia in accident environments. Because a launch pad or postlaunch explosion of the Space Transportation System vehicle (space shuttle) is a conceivable accident, the SVT plan included a series of tests that simulated the overpressure exposure the RTG and GPHS modules could experience in such an event. Results of these tests, in which we used depleted UO_2 as a fuel simulant, suggest that exposure to overpressures as high as 15.2 MPa (2200 psi), without subsequent impact, does not result in a release of fuel.

I. INTRODUCTION

The General-Purpose Heat Source (GPHS) is a modular component of a radioisotope thermoelectric generator (RTG) that will provide power for space missions. The first two flights will be the NASA Galileo and the ESA Ulysses (formerly International Solar-Polar) missions. The RTG provides electric power by using the heat of ^{238}Pu α-decay to create a temperature differential across a thermoelectric array. The Galileo spacecraft will use two RTGs, and the Ulysses will use a single RTG. Each RTG contains 18 GPHS modules.

A GPHS module contains four $^{238}PuO_2$-fueled clads and provides a total thermal output of 250 $W_{(t)}$ at the beginning of life. Each fueled clad consists of a $^{238}PuO_2$ pellet encapsulated in an iridium-alloy (0.3% tungsten) containment shell. Two fueled clads are held in a Fineweave-Pierced Fabric* (FWPF) graphite impact shell (GIS), and two GISs are contained within an FWPF aeroshell (Fig. 1). One of the goals of the GPHS module design was to minimize the release of plutonia in an accident environment.[1]

In the Galileo and Ulysses missions, a liquid-fueled Centaur rocket will be transported with each spacecraft in the cargo bay of the Space Transportation System vehicle (space shuttle). An Air Force Rocket Propulsion Laboratory analysis indicates that a launch explosion, fueled by the shuttle and Centaur propellants, would expose the RTG and GPHS modules to high overpressures.[2] Consequently, the Safety Verification Test (SVT) plan included a series of tests to determine the response of the GPHS components to such overpressures.[3]

II. THE TEST PROGRAM

The explosion overpressure tests simulated the overpressure exposure that a PuO_2-containing GPHS module would experience in a launch explosion. Twelve overpressure tests were conducted. In the first three tests

*Fineweave-Pierced Fabric 3-D carbon/carbon composite, a product of AVCO Systems Division, 201 Lowell St., Wilmington, MA 01887.

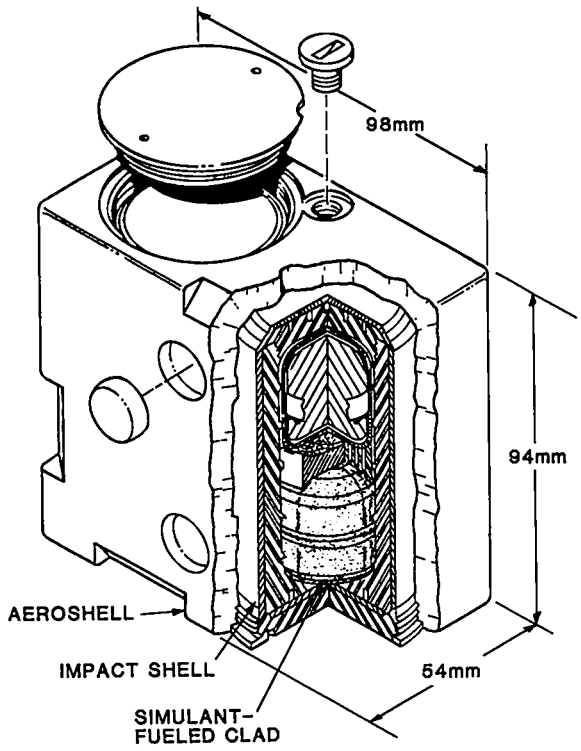

Fig. 1. Each GPHS module contains four $^{238}PuO_2$-fueled capsules.

(bare module tests or BMTs), bare GPHS modules were exposed to the overpressure environment. At that time, these were considered conservative tests, because we believed that the RTG housing would provide some protection to the GPHS modules. We had planned to test at incrementally higher overpressures (to a maximum of 13.8 MPa) in this test series, but the testing was suspended because an analysis of the DIRECT COURSE test (a 1-kt-equivalent nuclear simulation) suggested that the RTG converter housing increases rather than decreases damage to the GPHS modules in an explosion.[4] When the shock tube tests were resumed, a simulated RTG housing was included (converter segment tests or CSTs).

The CSTs were conducted to determine the effect of the RTG housing on the response of the GPHS modules and to more accurately simulate the actual explosion environment. The first two tests were similar in magnitude to BMT-2 and BMT-3 so that the effect of the housing could be determined. The remaining tests were conducted at incrementally higher overpressures.

A. Components

A fuel simulant of sintered uranium dioxide (depleted UO_2) was used in all of the tests because the test facility was not equipped to contain plutonium oxide. The bulk density and dimensions of each UO_2 pellet were adjusted to match the mass and configuration of an average plutonia fuel pellet. Other components are described below.

1. Bare Module Tests. The test object was a fully loaded GPHS module. One bulk graphite module, with the same external dimensions as the GPHS module, was placed above and another was placed below the test module. All FWPF components were flight-quality material and were machined to flight configurations. The iridium-alloy containment shells were also flight-quality units and were provided by the Mound Facility. Los Alamos National Laboratory fabricated the fuel pellets, encapsulated the pellets in the containment shells, and assembled the target components. Data describing the iridium and UO_2 components used in these tests are presented in Table I.

2. Converter Segment Tests. In the CSTs, a module stack identical to the BMT assembly was exposed to a blast wave acting through an RTG housing simulant. However, in CST-6-RTG-2, the module stack consisted of three fully loaded GPHS modules with a half-thickness bulk graphite module placed above and below.

Two different RTG simulants were used in the tests. In the first four CSTs, the RTG simulant was a C-shaped, 6.35-mm-thick aluminum-alloy (6061-T6) plate with a 7.62- × 17.27-cm window at the center. A 1.52-mm-thick aluminum (6061-T6) plate with flight-quality thermoelements and insulation (Fig. 2), provided by the General Electric Company (GE), was inserted into the window of the C-shaped plate and pop-riveted in place (Fig. 3).

In the last five CSTs, a cylindrical mockup with 1.52-mm-thick 6061-T6 aluminum walls (Fig. 4) was provided by GE to simulate the RTG housing. The cylinder contained flight-quality thermoelements and insulation in the center of the upstream and downstream sides. The remainder of the RTG simulant was filled with stainless steel weights to bring it to a mass and moment of inertia equal to a flight RTG. In CST-5-RTG-1, the stainless steel weights were 4.7-mm-thick plates of various sizes (as shown in Fig. 4). These plates were replaced with layers of stainless steel foil in the last four tests.

The fuel pellets used in CST-1, CST-2, and the CST-8-RTG-4 A-GIS were encapsulated in containment shells at Los Alamos National Laboratory. The remaining fuel pellets were encapsulated at the Savannah River Laboratory. The iridium and UO_2 components used in these tests are presented in Table I.

Table I. Components Used in the GPHS Explosion Overpressure Tests

Test	Capsule	Iridium Clad Vent Cup	Iridium Clad Blind Cup	UO_2 Pellet	Fueled Capsule Weight (g)
BMT-1	IRG-115	LR283-5	L265-8	62-100	208.236
and	IRG-116	LR284-3	LR284-2	62-101	201.766
BMT-2	IRG-117	LR284-8	LR284-5	62-94	208.077
	IRG-118	LR286-8	LR286-6	62-105	204.641
BMT-3	IRG-096	LR290-7	LR290-8	62-87	204.079
	IRG-097	LR292-7	LR271-7	62-81	202.698
	IRG-098	L294-5	LR301-5	62-76	199.760
	IRG-099	L294-7	LR288-5	62-68	201.563
CST-1	IRG-107	L265-2	L264-8	62-73	206.266
	IRG-108	L265-6	L265-5	62-84	204.179
	IRG-109	L266-6	LR292-8	62-74	199.710
	IRG-110	LR276-5	LR293-3	62-97	203.149
CST-2	IRG-125	LR320-4	LR319-5	62-113	209.107
	IRG-126	MER28-4	MER23-1	62-115	201.880
	IRG-127	MER24-6	MER24-1	62-116	200.871
	IRG-128	MER23-3	MER24-3	62-117	201.718
CST-3	L-12	X343-6	VR224R-1	63-07	203.004
	L-14	YR423-1	YR424-3	63-06	203.572
	L-16	YR420-4	YR420-5	63-15	203.344
	L-19	YR422-5	YR421-6	63-10	204.843
CST-4	L-9	ZR571-5	T103-1	62-118	204.591
	L-10	V211-4	TR125-5	63-04	204.574
	L-15	YR423-3	YR423-4	63-08	203.030
	L-23	Y412-1	Y416-5	63-13	200.706
CST-5-RTG-1	L-17	Z508-5	Z510-4	63-16	203.712
	L-18	TR129-6	Z505-6	63-09	202.963
	L-22	Z521-1	Z520-4	63-12	205.056
	L-24	Z563-3	Z560-2	63-14	203.266
CST-6-RTG-2[a]	M-10	5313	5335	85-11	202.434
	M-11	5334	5351	85-12	201.669
	M-12	5273	5124	85-13	202.019
	M-15	2361	5544	85-14	203.262
	M-9	5235	5333	85-10	205.648
	M-22	5405	5473	85-15	207.193
	M-23	5411	5475	85-27	206.575
	M-26	0172	0185	85-17	207.359
	M-8	5284	5331	85-09	203.630
	M-17	4294	5484	85-23	205.212
	M-18	5485	7313	85-21	205.136
	M-20	5384	5444	85-26	204.125
CST-7-RTG-3	M-30	TR132-1	TR423-2	85-30	202.689
	M-32	Z558-3	Z562-2	85-32	202.076
	M-34	Z562-5	Z558-2	85-34	201.835
	M-35	Z548-2	Z562-6	85-35	201.102
CST-8-RTG-4	IRG-132	Q806-3	MER26-2	62-122	202.082
	IRG-133	PR720-2	MER27-4	62-124	201.304
	M-24	5011	5015	85-16	207.325
	M-48	Z550-4	PR731-2	85-45	206.030
CST-9-RTG-5	M-40	Z562-1	Z545-3	85-37	205.260
	M-42	Z558-1	ZR571-2	85-39	206.878
	M-44	SR069-3	Z550-1	85-41	205.896
	M-46	ZR571-3	Z550-5	85-43	206.523

[a]A three-module stack was exposed.

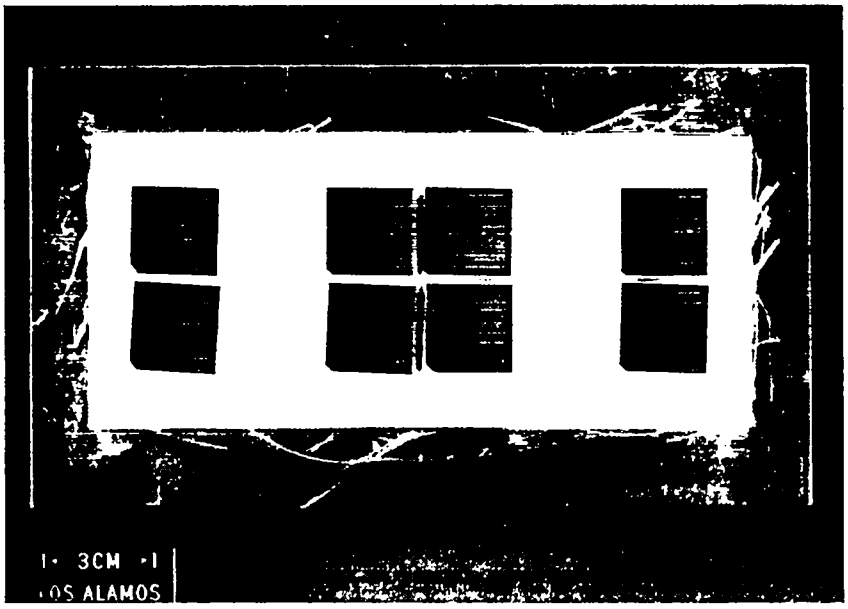

(a)

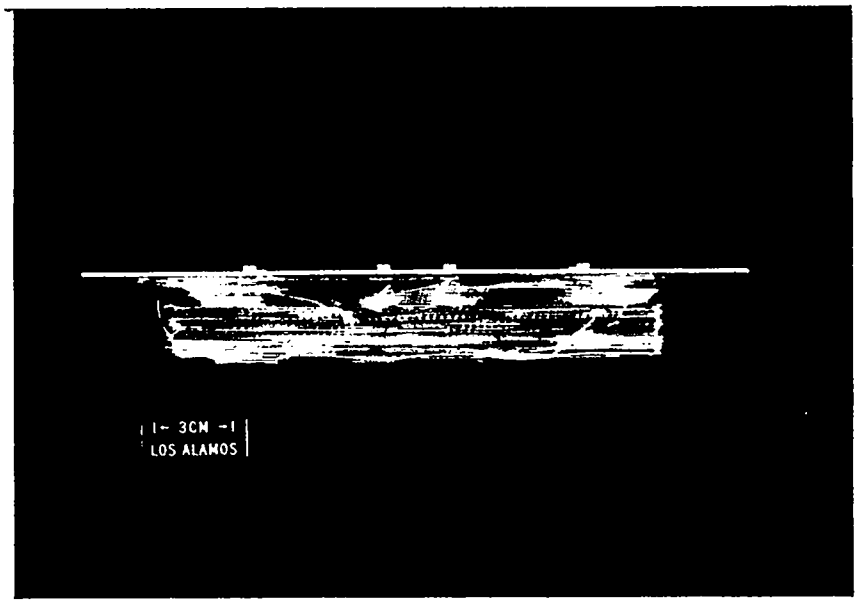

(b)

Fig. 2. The GE segment for the shock tube tests (C-shaped housing simulant) consisted of a 1.52-mm-thick aluminum (6061-T6) plate with flight-quality thermoelements and insulation attached; (a) face-on view and (b) overhead view.

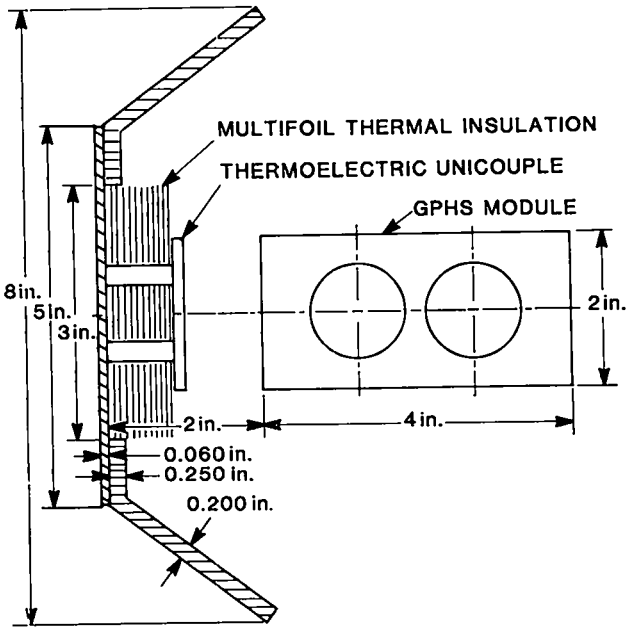

Fig. 3. The C-shaped housing simulant with GE segment in place (dimensions approximate).

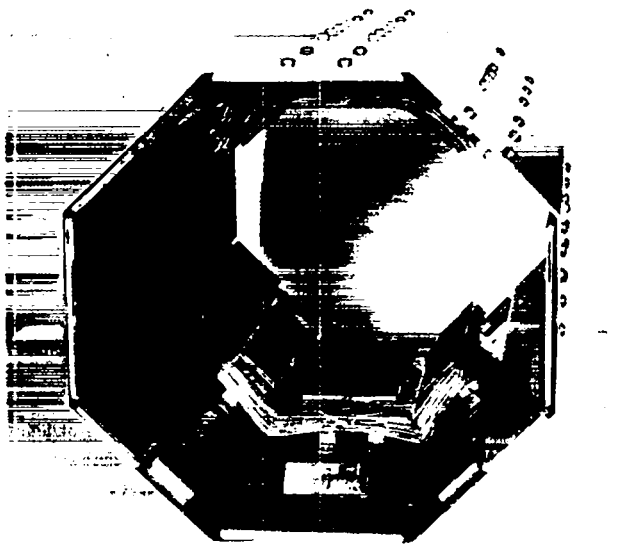

Fig. 4. The 1.52-mm-thick aluminum (6061-T6) GE cylindrical housing simulant contained flight-quality thermoelements and insulation in the center of the upstream and downstream sides.

B. Procedures

All of the overpressure tests were conducted at Sandia National Laboratories' (SNLA) Coyote III Test Area in Albuquerque, New Mexico. SNLA was responsible for charge calculation, fabrication, detonation, shock tube preparation, and shock tube diagnostics. Los Alamos was responsible for test section assembly and operation, flash x-ray setup, and posttest recovery and analysis.

In each test, the main shock tube was a seamless pipe of ASTM 53-Grade B steel, nominally 60.96 cm o.d. by 2.54 cm thick. A 175-cm-long test section (Fig. 5) containing the test object was bolted to the main shock tube. Pressure transducers mounted in the shock tube wall sensed the time of shock wave arrival and the static pressure time histories from which the overpressure at the test object location was calculated.

The total shock tube length varied, depending on the desired overpressure and impulse. Los Alamos specified the test parameters, and SNLA calculated the charge size and tube length required to achieve the desired conditions at the test object location. A large charge required a longer shock tube than would a smaller charge to achieve the same overpressure at the test object location. However, a larger charge and longer tube were necessary if a longer impulse was desired.

Before each test, the shock tube ends were sealed with aluminum foil and plastic, and a nitrogen gas flow to the furnace and shock tube was initiated. Flash x-ray units were positioned at the exit end of the shock tube so that velocity measurements of the test objects could be calculated based on test object positions and elapsed time. The x-ray units were triggered after a calculated delay time from detonation.

1. Bare Module Tests. In each test, the GPHS module was heated in a cylindrical furnace insulated with bulk graphite and carbon felt insulation. The module stack was placed in a graphite cradle suspended from the furnace lid. The temperature of the module stack was read directly from a Type K thermocouple inserted between the test module and the top bulk graphite module. When the test stack reached about 1110°C (about 20° above the target test temperature of 1091° C, the average temperature of clads in an on-pad RTG), a 2-min countdown was initiated. An explosive-actuated pin was retracted at about T −30 s to lower the furnace, leaving the heated stack suspended in the shock tube. A second explosive pin was detonated to release a counterweight steel plate that closed a sliding door over the retracted furnace to eliminate blast wave reflection from the furnace extension. The module stack cooled to the desired test temperature while the door was being closed.

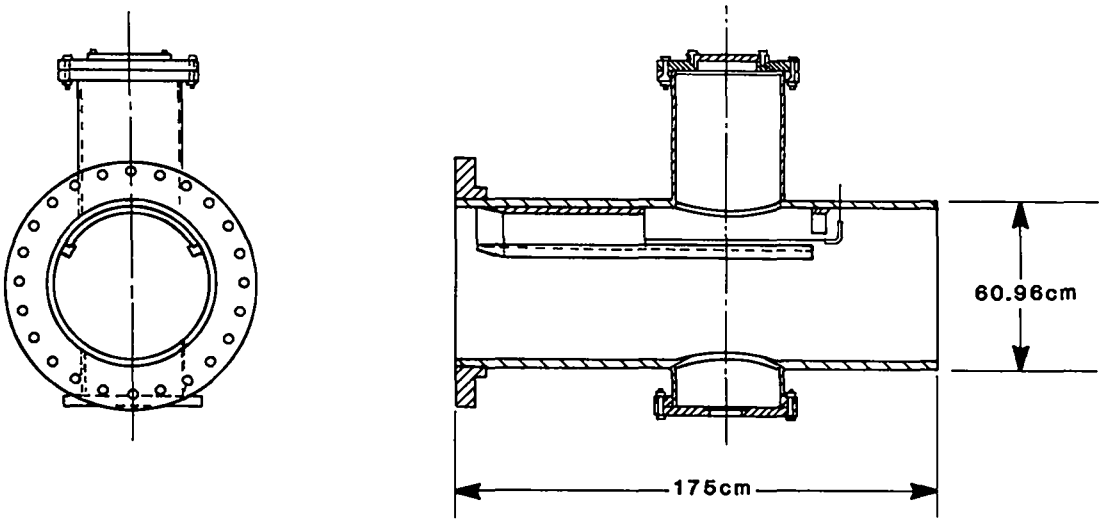

Fig. 5. The test assembly was contained in a seamless steel (ASTM 53-Grade B) test section bolted to the main shock tube.

An SNLA hand-packed Composition C-4 explosive (5% TNT), fitted with a point detonator, was detonated after test readiness was verified on a video monitor in the instrumentation bunker. The test objects were recovered from a vermiculite-filled catch tube by sifting the filler through 6.35-mm screens.

Recovered items were examined, photographed, and transported to Los Alamos for postmortem examination. The clads were photographed again at Los Alamos, x-rayed, and measured for deformation. The most deformed clad in each test was selected for metallography and was sectioned; the fuel simulant was observed and photographed.

2. Converter Segment Tests. In the first four CSTs, the C-shaped housing simulant was attached to an aluminum bracket mounted to the sliding door. The test procedures were identical to those used in the BMTs, except that the sliding door was closed by an automatic electric winch, positioning the RTG simulant with thermoelements and insulation 3.81 cm upstream from the test module (Fig. 6).

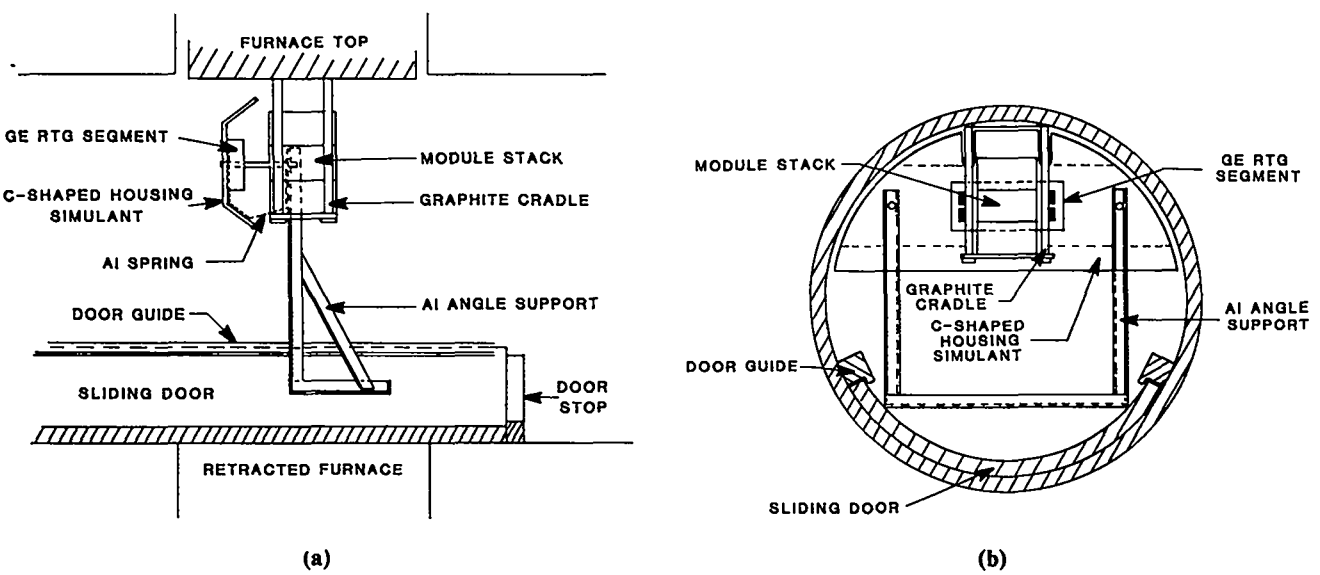

Fig. 6. Shock tube test setup with C-shaped RTG simulant; (a) section view and (b) end view.

After the clads were recovered and transported to Los Alamos, they were grit-blasted with 10-μm alumina abrasive to remove the adhering vermiculite. The clads were then measured for deformation, and the most deformed capsule in each test, as well as any breached clads, were selected for particle size analysis of the fuel and for metallography. Urania particle size data are listed in Table II. Specimens for metallography were cut from the vent and weld shield cups of the capsules. Grain sizes of the iridium cups are listed in Table III.

In the last five CSTs (cylindrical housing simulant), the module stack was heated in a stationary furnace insulated with alumina, Marinite, and Fiberfrax Durablanket* insulation. The test stack was mounted to a removable furnace base with a graphite holder. An extended air cylinder, with graphite insulating blocks attached to the end of the piston, held the module stack in the furnace during heating. When the stack reached the desired temperature, it was lowered with the furnace base into the converter simulant at the center of the shock tube by remote operation of the air cylinder.

The temperature of the module stack was not measured directly when it was in the test position. Instead, the impact temperature was inferred from prior calibration measurements. After the module stack was lowered, an electric winch pulled the sliding door closed under the furnace cavity to reduce blast wave reflection at the test object location (Fig. 7). Except in CST-9-RTG-5, a Composition C-4 explosive was detonated after test readiness was verified on a video monitor in the instrument bunker. In CST-9-RTG-5, a Los Alamos-cast and -machined Composition B explosive (40% TNT) was detonated with a plane-wave generator. The catch tube filler in CST-5-RTG-1 was vermiculite, which was sifted through 6.35-mm screens. The test objects in the final four CSTs were recovered from a sawdust-filled catch tube by sifting the filler through 12.7-mm screens.

The sawdust was substituted for vermiculite in the last four tests because fueled clads recovered from previous tests exhibited signs of possible chemical interactions with the vermiculite, and we felt that these clads should not be used in follow-on tests. We chose sawdust as a vermiculite substitute because of its availability, light weight, and high carbon content. In addition, no chemical interaction between sawdust and iridium had been seen in a series of Los Alamos tests in which fueled clads were heated to 1091°C and cooled in a sawdust-filled steel drum.

*Fiberfrax Durablanket insulation, a product of Carborundum Company, Insulation Division, P.O. Box 808, Niagra Falls, NY 14302.

III. RESULTS

The conditions and results of each test are summarized in Tables IV and V. Details of the individual tests and postmortem examinations are given below.

A. Bare Module Test 1

In the first shock tube overpressure test (BMT-1), an explosive charge of 5.9 kg (13 lb) was detonated at the end of a 20.1-m-long shock tube, exposing the heated (1091 ± 5°C) module stack to a blast wave of 1.4 ± 0.07 MPa (200 ± 10 psi) overpressure and 8.4 ± 1.4 kPa · s (1.22 ± 0.2 psi · s) impulse. The module penetrated 0.8 m into the catch tube. The only external damage to the module consisted of pitting on the surface facing the blast wave and a minor chip on one corner. The chip apparently occurred when the test module collided with one of the bulk graphite modules.

Radiographic examination of the test module revealed that neither the impact shells nor the capsules had been damaged. Fueled clad diametral measurements ranged from a maximum:minimum diameter ratio (M/m) of 1.001 to an M/m of 1.003. Because the clads in this test module were to be used in the next overpressure test, they were not sectioned.

B. Bare Module Test 2

In this test (BMT-2), we heated the BMT-1 test module to 1093 ± 5°C, and we detonated 27.2 kg (60 lb) of explosive at the end of a 20.1-m-long shock tube to create a blast wave of 5.1 ± 0.21 MPa (735 ± 30 psi) overpressure and 22.1 ± 2.8 kPa · s (3.2 ± 0.4 psi · s) impulse. The test module was driven 1 m into the catch tube. The recovered module is shown in Fig. 8. The aeroshell fractured on a broad face that had been oriented parallel to the blast direction. The C-GIS (Fig. 9) was broken and fueled clad IRG-118 was visible. The A-GIS (Fig. 10), which was on the blast side of the module, appeared undamaged.

The clads were removed from the impact shells and photographed (Fig. 11). None of the clads breached. Diametral measurements indicated an M/m ranging from 1.002 to 1.029. Capsule IRG-118, which had the greatest local deformation, was selected for microscopic examination. The IRG-118 fuel simulant (Fig. 12) was broken into relatively large pieces.

Table II. GPHS Explosion Overpressure Tests—Urania Particle Size Analyses of Selected Clads

Particle Size[a] (μm)	CST-1 (Clad 1) 5.1 MPa	CST-2 (IRG-128) 7.1 MPa	CST-3 (L-12) 11.6 MPa	CST-4 (L-10) 12.1 MPa	CST-5 (L-24) 12.5 MPa	CST-7 (M-35) 12.9 MPa	CST-8 (IRG-133) 2.96 MPa	CST-9 (M-46)[b] 15.3 MPa	CST-9 (M-40) 15.3 MPa
+6000	0.6774	0.9263	0.3567	0.8407	0.8407	0.8765	0.9009	0.1276	0.3726
−6000 +2000	0.1836	0.0437	0.1905	0.0580	0.0701	0.0818	0.0556	0.3027	0.2450
−2000 +841	0.0850	0.0179	0.2794	0.0572	0.0481	0.0242	0.0274	0.2912	0.2076
−841 +420	0.0308	0.0058	0.1094	0.0394	0.0212	0.0075	0.0067	0.1374	0.0968
−420 +177	0.0141	0.0033	0.0379	0.0228	0.0121	0.0045	0.0044	0.0825	0.0500
−177 +125	0.0024	0.0007	0.0140	0.0037	0.0023	0.0011	0.0011	0.0177	0.0081
−125 +74	0.0024	0.0009	0.0054	0.0037	0.0023	0.0011	0.0013	0.0179	0.0069
−74 +44	0.0012	0.0004	0.0022	0.0018	0.0009	0.0007	0.0008	0.0080	0.0033
−44 +30	0.0009	0.0003	0.0015	0.0010	0.0008	0.0005	0.0006	0.0052	0.0029
−30 +20	0.0004	0.0001	0.0007	0.0005	0.0002	0.0004	0.0003	0.0019	0.0013
−20 +10	0.0005	0.0002	0.0007	0.0006	0.0003	0.0006	0.0003	0.0026	0.0017
−10	0.0013	0.0004	0.0017	0.0010	0.0008	0.0010	0.0006	0.0053	0.0039
1.00 (max)	0.000169	0.000023	0.000218	0.000141	0.000108	0.000076	0.000030	0.000140	0.000235
2.00 (max)	0.000152	0.000038	0.000327	0.000318	0.000126	0.000056	0.000091	0.000273	0.000578
3.00 (max)	0.000199	0.000052	0.000293	0.000149	0.000133	0.000084	0.000117	0.000896	0.000737
4.00 (max)	0.000263	0.000046	0.000066	0.000173	0.000085	0.000134	0.000101	0.001021	0.000536
5.00 (max)	0.000128	0.000059	0.000100	0.000095	0.000066	0.000146	0.000054	0.001056	0.000390
6.00 (max)	0.000101	0.000035	0.000123	0.000018	0.000069	0.000078	0.000044	0.000668	0.000248
7.00 (max)	0.000032	0.000035	0.000039	0.000000	0.000055	0.000069	0.000026	0.000327	0.000113
8.00 (max)	0.000096	0.000030	0.000234	0.000043	0.000027	0.000021	0.000052	0.000487	0.000337
9.00 (max)	0.000068	0.000011	0.000083	0.000000	0.000077	0.000088	0.000019	0.000174	0.000359
10.00 (max)	0.000093	0.000030	0.000228	0.000085	0.000053	0.000282	0.000076	0.000238	0.000329

[a]Values are expressed as a fraction of total pellet weight.
[b]Recovered weight = 64.3809 g.

Table III. Average Grain Size of CST Clads

Clad	Test	Cup	Average Grains per 0.635-mm Nominal Wall Thickness
Clad 1	CST-1	Vent	21.9
		Shield	23.1
IRG-128	CST-2	Vent	21.8
		Shield	23.8
L-12	CST-3	Vent	26.2
		Shield	23.2
L-10	CST-4	Vent	27.8
		Shield	31.7
L-24	CST-5-RTG-1	Vent	28.8
		Shield	26.3
L-18	CST-5-RTG-1	Vent	27.2
		Shield	26.3
M-35	CST-7-RTG-3	Vent	24.2
		Shield	29.8
IRG-133	CST-8-RTG-4	Vent	26.8
		Shield	23.2
M-40	CST-9-RTG-5	Vent	26.3
		Shield	23.3

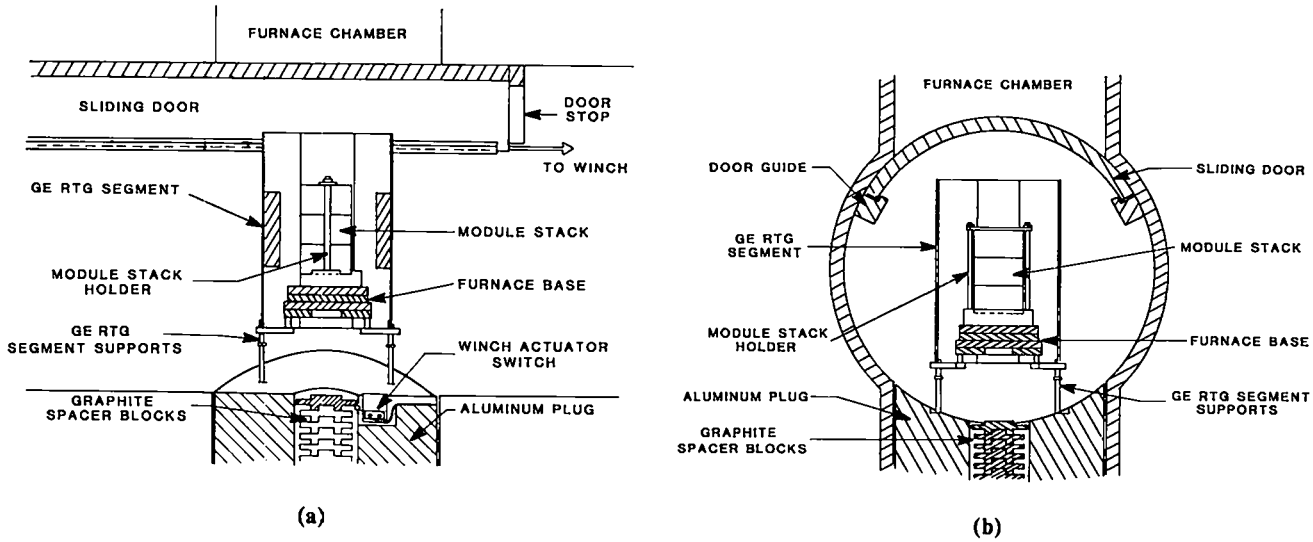

Fig. 7. Shock tube test setup with cylindrical RTG simulant; (a) section view and (b) end view.

Table IV. GPHS Explosion Overpressure Tests—Conditions

Test	Overpressure (MPa)	Impulse (kPa · s)	Tube Length (m)	Charge (kg)	Catch Medium
BMT-1	1.4 ± 0.07	8.4 ± 1.4	20.1	5.9 C-4	vermiculite
BMT-2	5.1 ± 0.21	22.1 ± 2.8	20.1	27.2 C-4	vermiculite
BMT-3	7.4 ± 0.34	25.9 ± 3.5	20.1	49.9 C-4	vermiculite
CST-1	5.1 ± 0.48	22.1 ± 2.8	17.7	27.2 C-4	vermiculite
CST-2	7.1 ± 0.69	25.9 ± 5.2	18.6	48.1 C-4	vermiculite
CST-3	11.6 ± 2.1	29.0 ± 5.5	20.7	81.0 C-4	vermiculite
CST-4	12.2 ± 1.2	27.6 ± 5.5	18.9	116.4 C-4	vermiculite
CST-5-RTG-1	12.5 ± 1.2	27.6 ± 5.5	18.9	116.4 C-4	vermiculite
CST-6-RTG-2	13.5 ± 1.3	23.2 ± 4.8	14.9	136.2 C-4	sawdust
CST-7-RTG-3	12.9 ± 2.5	23.5 ± 4.8	14.6	125.8 C-4	sawdust
CST-8-RTG-4	2.96 ± 0.28	14.5 ± 2.8	19.5	12.5 C-4	sawdust
CST-9-RTG-5	15.3 ± 1.5	16.6 ± 3.5	14.6	93.1 Comp B	sawdust

C. Bare Module Test 3

In the third test, a charge of 49.9 kg (110 lb) was detonated at the end of a 20.1-m-long shock tube to create a blast wave of 7.4 ± 0.34 MPa (1070 ± 50 psi) overpressure and 25.9 ± 3.5 kPa · s (3.75 ± 0.5 psi · s) impulse at the test module location. The blast wave stripped the graphite components from the heated (1095 ± 5°C) test clads, three of which were recovered approximately 3.0 m deep in the catch tube. A fourth capsule penetrated the plywood bulkhead at the rear of the catch tube and came to rest about 10 cm behind it (in dirt). None of the clads breached. Fragments of the FWPF components (aeroshell and impact shells) were recovered throughout the catch tube.

The four fueled clads are shown in Fig. 13. Posttest identification of the specific fueled clads was not possible, so they were labeled A, B, C, and D. Capsule D had penetrated the plywood bulkhead, but it did not exhibit the highest strain. Capsule C, which was sectioned before a gross diametral strain could be determined, had a local bend strain of −4.7%. The diametral strains of the other fueled clads ranged from 1.003 to 1.020. The UO_2 pellet removed from capsule C is shown in Fig. 14. One end of the pellet was fragmented.

D. Converter Segment Test 1

The first shock tube overpressure test with an intervening RTG housing simulant was conducted to evaluate the effect of such a housing on module damage. A charge of 27.2 kg (60 lb) was detonated at one end of a 17.7-m-long shock tube to create a blast of 5.1 ± 0.48 MPa (736 ± 70 psi) overpressure and 22.1 ± 2.8 kPa · s (3.2 ± 0.4 psi · s) impulse at the test module location. The FWPF graphite components were completely stripped away from the four simulant-fueled clads, which were recovered at a catch tube depth of about 2.2 m. None of the clads breached. We recovered 30 pieces of the GE segment (with an average weight of 2.43 g) and small fragments of the thermoelements and insulation from the catch tube.

The four fueled clads are shown in Fig. 15. Posttest identification of the specific fueled clads was not possible, so the clads were labeled 1, 2, 3, and 4, in the order they were recovered. The fueled clad diametral strains ranged from 1.022 to 1.069, with Clads 1 and 3 showing the greatest M/m. Clad 1 was sectioned and the urania was sized. Particle size data are shown in Table II.

Macroscopic examination of Clad 1 revealed a deep crater (Fig. 16) on the vent cup radius. Subsequent microscopic examination revealed that at its deepest point, the crater penetrated less than 25% of the total wall thickness. Significant grain elongation occurred in the cratered area (Fig. 17).

Both iridium cups were fine grained. The average grain size of the vent cup was 21.9 grains/thickness, and the average grain size of the weld shield cup was 23.1 grains/thickness (See Table III). No areas of grain coarsening were observed on either cup.

Examination of the capsule weld revealed a normal microstructure with full penetration. The capsule vent (Fig. 18) was negligibly deformed and contained no mechanical defects. The vent assembly and decontamination cover welds were fine grained.

Table V. GPHS Explosion Overpressure Tests—Results

Test	Overpressure and Impulse	Response	Range M/m[a]	Average Catch Medium Penetration (m)
BMT-1	1.4 ± 0.07 MPa 8.4 ± 1.4 kPa · s	No graphite damage	1.001-1.003	0.8
BMT-2	5.1 ± 0.21 MPa 22.1 ± 2.8 kPa · s	Minor graphite damage	1.002-1.029	1.0
BMT-3	7.4 ± 3.4 MPa 25.9 ± 3.5 kPa · s	Graphite stripped Free-flight clads	1.003-1.020	3.0
CST-1	5.1 ± 0.48 MPa 22.1 ± 2.8 kPa · s	Graphite stripped Free-flight clads	1.022-1.069	2.2
CST-2	7.1 ± 0.69 MPa 25.9 ± 5.2 kPa · s	Graphite stripped Free-flight clads	1.018-1.059	3.9
CST-3	11.6 ± 2.1 MPa 29.0 ± 5.5 kPa · s	Graphite stripped Free-flight clads	1.052-1.113	6.1
CST-4	12.2 ± 1.2 MPa 27.6 ± 5.5 kPa · s	Graphite stripped Free-flight clads	1.009-1.094	7.5
CST-5-RTG-1	12.5 ± 1.2 MPa 27.6 ± 5.5 kPa · s	Graphite stripped Free-flight clads	1.082-1.104[b]	5.6
CST-6-RTG-2	Indeterminate	See Table VI	See Table VI	N/A
CST-7-RTG-3	12.9 ± 2.5 MPa 23.5 ± 4.8 kPa · s	Graphite stripped Free-flight clads	1.038[c]	5.6
CST-8-RTG-4	2.96 ± 0.28 MPa 14.5 ± 2.8 kPa · s	Retained in graphite	1.004-1.055	1.0
CST-9-RTG-5	15.3 ± 1.5 MPa 16.6 ± 3.5 kPa · s	Graphite stripped Free-flight clads	1.066[c]	6.0

[a]Maximum:minimum diameter ratio.
[b]Three clads recovered integral.
[c]One clad recovered integral.

E. Converter Segment Test 2

A second test with an intervening RTG housing simulant (CST-2) was conducted at a slightly higher overpressure. A blast of 7.1 ± 0.69 MPa (1028 ± 100 psi) overpressure and 25.9 ± 5.2 kPa · s (3.75 ± 0.5 psi · s) impulse was calculated at the test module location when a 48.1-kg (106-lb) charge was detonated at the other end of the 18.6-m-long shock tube. The blast stripped the FWPF graphite components from the four fueled clads but none of the clads breached. The clads were recovered at a catch tube depth of about 3.9 m. We also recovered 30 pieces of the GE RTG segment, averaging 1.45 g, and small pieces of the thermoelements and insulation.

The four fueled clads are shown in Fig. 19. We were able to identify specific fueled clads by comparing pretest and posttest clad vent photographs. The fueled clad diametral strains ranged from 1.018 to 1.059. Clad IRG-128, with an M/m of 1.059, was sectioned and the fuel simulant was sized. See Table II for particle size data.

Macroscopic examination of the exterior of clad IRG-128 did not reveal any cracks, craters, or other defects. Microscopic examination of the capsule weld revealed a porous but otherwise acceptable microstructure. The weld bead was narrow and fully penetrated the capsule wall. Both iridium cups were uniformly fine grained (Table III).

The capsule vent (Fig. 20) was undeformed and contained no mechanical defects. The vent assembly and decontamination cover welds were free of grain growth.

F. Converter Segment Test 3

In CST-3, the charge was increased to 81 kg (178.5 lb) to generate a blast of 11.6 ± 2.1 MPa (1684 ± 300 psi) overpressure and 29.0 ± 5.5 kPa · s (4.2 ± 0.8 psi · s) impulse at the test module location. Time-of-arrival data from pressure transducers indicated an accelerating shock wave in the 20.7-m-long shock tube. This phenomenon, probably caused by side-wall turbulence, increased the uncertainty of the calculated overpressure. The FWPF graphite components were again stripped away, but none of the clads breached. The clads were recovered about 6.1 m deep in the vermiculite. We recovered 35 pieces of the GE segment with an average weight of 0.52 g. Small pieces of the thermoelements and insulation were also recovered.

The four fueled clads are shown in Fig. 21. The clads, which were identified from laser etchings on the clad exteriors, had diametral strains ranging from 1.052 to 1.113. Clad L-12, with an M/m of 1.080, was selected for sectioning because a deep crater was observed on the weld shield cup. Particle size data are listed in Table II.

Microscopic examination of clad L-12 revealed that the crater on the weld shield cup penetrated 38% of the wall thickness (Fig. 22). The capsule wall within the crater displayed significant ductility (Fig. 23).

Although the closure weld (Fig. 24a) was completely free of porosity and other defects, it had an abnormal microstructure (Fig. 24b). While it is unclear how such an unusual microstructure could form, the orientation of long columnar grains along the weld centerline would substantially reduce the tensile strength of the weld. No cracks or other defects were observed at any point on the weld surface.

As in previous CST clads, the iridium cups were uniformly fine grained (Table III), and the capsule vent was undeformed and free of mechanical defects (Fig. 25). However, a small, nonpenetrating crack was observed on one side of the vent assembly (Fig. 26). The vent cover and assembly welds were completely free of abnormal grain growth.

G. Converter Segment Test 4

In this test, a 116.4-kg (256.5-lb) charge was detonated at the end of an 18.9-m-long shock tube to produce a blast of 12.2 ± 1.2 MPa (1750 ± 175 psi) overpressure and 27.6 ± 5.5 kPa · s (4.0 ± 0.8 psi · s) impulse at the test module location. The clads were recovered at a vermiculite depth of about 7.5 m; none were breached. Small impact craters, ranging in size from pin points up to 6.4 mm^2, were observed on all of the clad exteriors; no iridium cracking was observed within or adjacent to any of the craters. Only eight pieces of the GE segment, with an average weight of 0.99 g, were recovered from the catch tube. No pieces of the thermoelements or insulation were recovered.

On an x-ray film, one fueled clad appeared approximately 3.2 m from its original test position. The x-ray geometry is shown in Fig. 27. If we assume a delay time of 12 ms from detonation and use a 4.3-ms shock wave arrival time at the test position, the clad velocity was approximately 414 m/s (neglecting acceleration).

The clads, shown in Fig. 28, were identified from laser etchings on the clad exteriors. The diametral strains ranged from 1.009 to 1.094. Clad L-10, with an M/m of 1.094, was sectioned. Particle size data are shown in Table II.

A large crater occurred on the blind cup of capsule L-10. A transverse section, which contained the large crater and a smaller indentation (Fig. 29), was removed for metallography. Examination of the large crater revealed that it penetrated more than 70% of the wall thickness (Fig. 30). The crater rim exhibited a small amount of internal grain boundary cracking. The capsule wall within the crater (Fig. 31) was severely deformed with significant grain elongation and little recrystallization. The small indentation (Fig. 32) was similar to the large crater, differing only in size and in the symmetry of deformation.

A cratered section of the L-10 vent cup (Fig. 33) was also removed for examination. A large crater in this cup penetrated approximately 40% of the wall thickness. The deformation produced a remarkable pattern of internal grain boundary cracks (Fig. 34) on one side of the crater.

The L-10 closure weld had no observable defects and had a typical microstructure. Both of the L-10 iridium cups were uniformly fine grained (Table III).

Examination of a vent cross section (Fig. 35) revealed that the vent was undeformed and free of mechanical defects. However, both sides of the vent assembly weld were cracked (Fig. 36). No abnormal grain growth occurred at the vent assembly or decontamination cover welds.

H. Converter Segment Test 5

In CST-5-RTG-1, the C-shaped converter simulant used in the first four CSTs was replaced with a cylindrical RTG simulant. As in CST-4, a charge of 116.4 kg (256.5 lb) was detonated at the end of an 18.9-m-long shock tube. A blast of 12.5 ± 1.2 MPa (1815 ± 180 psi) overpressure and 27.6 ± 5.5 kPa · s (4.0 ± 0.8 psi · s)

impulse impacted the heated (1091 ± 10°C) module stack suspended inside the simulated RTG. The FWPF graphite components were stripped from the clads, three of which were recovered intact at a depth of about 5.6 m. The fourth clad, recovered 9.0 m into the catch tube, breached. This clad was embedded in a plywood bulkhead that separated the dirt backfill from the catch tube media. Approximately 90 pieces of the RTG simulant, with an average weight of 0.59 g, were recovered. Most of the 4.7-mm-thick stainless steel weight segments and a few small pieces of thermoelements were also recovered.

All four clads were recorded on the x-ray films. The images showed that the capsules were integral and were close to a spinning high-density fragment. We believe that the high-density fragment, identified as a stainless steel weight, collided with one of the clads. This collision breached the clad and accelerated it, so that it penetrated the catch media much deeper than did the other clads. Clad velocities determined from the x-ray films (Fig. 37) ranged from about 409 to 424 m/s (neglecting acceleration time).

The four fueled clads are shown in Fig. 38. Diameter ratios of the integral clads ranged from 1.082 to 1.104. Clad L-24, with an M/m of 1.104, was sectioned and submitted for particle size analysis. Urania particle size data are shown in Table II.

Metallographic specimens were removed from both of the L-24 iridium cups. Examination of a severely deformed shield cup section (Fig. 39) revealed slight surface gouging and an unusual amount of grain elongation (Fig. 40). Similar grain elongation was observed in a deformed section of the vent cup (Fig. 41). Both cups were uniformly fine grained (Table III). The closure weld did not contain any observable defects and had an acceptable microstructure.

The capsule vent (Fig. 42) was not significantly deformed and was free of mechanical defects. However, one side of the vent assembly weld (Fig. 43) was cracked. The vent cover and assembly welds were free of abnormal grain growth.

Clad L-18, which struck the plywood, had a total breach area of 155.1 mm^2 through which approximately half of the fuel was released. A cross section of the capsule breach (Fig. 44) was carefully examined. A notable feature of this section was the deep gouging and surface cracking observed mainly on one side (vent cup radius, toward weld) of the breach (Fig. 45). Both sides of the fracture had a brittle, intergranular appearance (Fig. 46) with only slight grain elongation. Significant grain elongation (Fig. 47) did, however, occur in other areas of the weld shield cup.

Examination of a mildly deformed vent cup section (Fig. 48) revealed a deep crack that penetrated 80% of the capsule wall. The crack was intergranular and originated on the interior surface.

Both L-18 iridium cups were uniformly fine grained (Table III). The closure weld was defect free and had an acceptable microstructure.

Examination of the capsule vent revealed that it had been severely deformed (Fig. 49). The vent assembly and decontamination cover welds had very fine-grained microstructures.

I. Converter Segment Test 6

In the sixth CST, we generated a blast of 13.5 ± 1.3 MPa (1962 ± 190 psi) overpressure and 23.2 ± 4.8 kPa · s (3.36 ± 0.7 psi · s) impulse at the test module location. In order to have an adequate supply of overpressure-tested clads available for sequential tests, the test assembly consisted of a 3-module stack containing 12 simulant-fueled capsules. One bulk graphite half-module was placed above and another was placed below the stack. The catch tube was filled with sawdust, instead of vermiculite, to avoid a suspected chemical interaction of the iridium and vermiculite. The stainless steel weights in the RTG simulant were also replaced with layers of stainless steel foil to eliminate the possibility of clad failure from collision with one of the high-density weights.

The test assembly was not exposed to the intended overpressure. Instead, the module stack remained in the furnace and was ejected through the top of the furnace extension. Apparently, a thermocouple inserted into the top bulk graphite half-module failed to release, causing the module stack to become wedged in the furnace. However, we had no evidence that the module stack had remained in the furnace. Meanwhile, the video monitor in the instrumentation bunker showed the actuation of the winch, indicating that the air cylinder piston had lowered, but a cable connecting the winch to the sliding door failed before the door was completely closed. The countdown was placed on hold while the decision was made to conduct the test with the sliding door only partially closed.

Test debris was scattered over a wide area as shown in Fig. 50. We recovered all clads except for two from the bottom module, A-GIS (open) and C-GIS (blind). Four of the recovered fueled clads were still retained in graphite as shown in Fig. 51. Six clads were recovered bare, three of which were integral (Fig. 52). The remaining breached clads are shown in Fig. 53. All clads were positively identified from laser etchings on clad exteriors. Results from this test are summarized in Table VI. No urania particle size data were obtained.

Table VI. CST-6-RTG-2 Results

Clad Location	Clad	Recovery Condition	M/m	Breach Area (mm^2)	Fuel Released (g)
Top Module					
A-GIS (blind)	M-10	Integral (in GIS)	1.033	N/A	N/A
(open)	M-11	Integral (in GIS)	1.106	N/A	N/A
C-GIS (blind)	M-12	Integral (in GIS)	1.011	N/A	N/A
(open)	M-15	Integral (bare)	1.026	N/A	N/A
Middle Module					
A-GIS (blind)	M-9	Integral (in GIS)	1.048	N/A	N/A
(open)	M-22	Breached (bare)	---	Not measurable	113.8 (75%)
C-GIS (blind)	M-23	Integral (bare)	1.100	N/A	N/A
(open)	M-26	Integral (bare)	1.015	N/A	N/A
Bottom Module					
A-GIS (blind)	M-8	Breached (bare)	---	123.8	5.752 (2.8%)
(open)	M-17	Not recovered	---	---	---
C-GIS (blind)	M-18	Not recovered	---	---	---
(open)	M-20	Breached (bare)	---	Not measurable	150.3 (100%)

J. Converter Segment Test 7

CST-7-RTG-3 was a second attempt at exposing the GPHS RTG simulant to a nominal 13.8 MPa (2000 psi) overpressure. The test setup was similar to CST-6-RTG-2 with the following exceptions:

(1) Only a single test module containing four simulant-fueled clads was exposed.

(2) A thermocouple was suspended between the RTG simulant and the module stack to verify test stack position.

(3) An indicator was installed to verify complete door closure.

(4) A thermocouple was not inserted in the top bulk graphite module of the module stack. Instead, stack temperature was estimated by extrapolating from furnace temperature and data of previous tests.

We detonated 125.8 kg (277 lb) of explosive at the end of a 14.6-m-long shock tube to create a blast wave of 12.9 ± 2.5 MPa (1873 ± 360 psi) overpressure and 23.5 ± 4.8 kPa · s (3.4 ± 0.7 psi · s) impulse at the test module location. Time-of-arrival data indicated an accelerating shock wave, probably due to a turbulent or nonplanar shock front. This shock wave phenomenon increased the uncertainty in the calculated overpressure and may have significantly affected the test module response.

Clad M-35 from the open end of the C-GIS was recovered integral at a sawdust depth of 5.6 m (Fig. 54). Clad M-30 from the blind end of the A-GIS and six iridium fragments were recovered at a depth of about 3.5 m. Clad M-30 (Fig. 55) was breached, and over half of the fuel simulant had been released. The total recovered weight of the six clad fragments was 45 g. The two remaining fueled clads were not recovered. We believe that misalignment of the shock tube and catch tube before the test and shock tube movement during the test caused these clads to miss the catch tube.

The six clad fragments ranged in size from 9.37 mm^2 to 28.9 mm^2. All of the fragments contained deep striations and cracks on the exterior surfaces, suggesting impact against a large object or by high-velocity metal fragments. The clad fragment containing the deepest striations (Fig. 56) was selected for scanning electron microscope (SEM) examination.

Macroscopic examination of the fragment exterior revealed numerous surface cracks and deep gouges containing deposits of unknown origin. Microscopic analysis of one of the cracks (Fig. 57) indicated the presence of only iridium in the crack (Fig. 58). Microscopic analysis of a gouge (Fig. 59a) indicated the presence of both iridium and iron (Fig. 60). Elemental dot-mapping of the gouge clearly identified the iron (Fig. 59b) and iridium (Fig. 59c) areas. The analyses show that iron deposits were present in striations on the clad exterior; no iron was detected in cracks that postdated the striations. These results indicate that the clads were either struck by steel fragments or were thrown against the shock tube or catch tube walls.

Clad M-35, with an M/m of 1.038, was sectioned and the fuel simulant was sized. Urania particle size data are listed in Table II. Macroscopic examination of clad M-35 revealed a 1-cm-diameter dent and a small fragment puncture, typical of craters observed in other CST clads, on the vent cup radius. A section of the M-35 clad, containing the small crater, was submitted for electron microprobe analysis to identify the material in the crater. The analysis indicated that the principal constituents were aluminum and silicon, with lower concentrations of potassium, calcium, and iron. The x-ray spectrum produced was similar to that from clay minerals such as orthoclase.

A deformed section of the M-35 vent cup (Fig. 61) revealed slight grain elongation along the external surface and a reduction in thickness of about 27%. The capsule weld (Fig. 62) was unusually coarse grained, but it fully penetrated the capsule wall. Both iridium cups were uniformly fine grained (Table III).

K. Converter Segment Test 8

CST-8-RTG-4 was designed to determine the minimum overpressure at which the graphite is stripped away from the fueled clads. A charge of 12.5 kg (27.5 lb) was detonated at one end of a 19.5-m-long shock tube to create a blast wave of 2.96 ± 0.28 MPa (429 ± 40 psi) overpressure and 14.5 ± 2.76 kPa · s (2.1 ± 0.4 psi · s) impulse at the test module location. Test setup and procedures were identical to those in CST-7-RTG-3, except that two simulant-fueled Light Weight Radioisotope Heater Units (LWRHUs) mounted to the side walls of the shock tube were also exposed to the blast wave.

The graphite was not stripped from the fueled clads. The test module, recovered at a sawdust depth of 1 m, had two cracks coincident with the A-GIS major diameter on each side of the broad faces of the aeroshell (Fig. 63). All graphite remained in place, including the module closure caps. The A- and C-GISs were cracked (Fig. 64) and the carbon-bonded carbon-filament (CBCF) graphite insulation was about 50% powdered. We recovered 28 fragments of the RTG simulant, with a total weight of 898.78 g, from the catch media; the RTG fragments ranged in weight from 0.57 to 164.14 g.

The four fueled clads are shown in Fig. 65. The clad deformations ranged from 1.004 to 1.055. Clad IRG-133, with an M/m of 1.055, was sectioned and the simulant fuel was sized (Table II). Macroscopic examination of the exterior of IRG-133 did not reveal any cracks, craters, or other defects. Microscopic examination of the capsule weld revealed an acceptable microstructure. The weld bead was narrow and fully penetrated the capsule wall. Both iridium cups were uniformly fine grained (Table III).

The simulant-fueled LWRHUs (Fig. 66) were recovered integral from the catch tube at a depth of about 2 m. The external casing on each unit was slightly pitted and gouged, and the insulation was slightly cracked, but no significant deformation occurred.

L. Converter Segment Test 9

CST-9-RTG-5 was a third attempt at exposing the GPHS module to a nominal 13.8 MPa (2000 psi) overpressure. To minimize a reoccurrence of the blast wave turbulence observed in CST-7-RTG-3, we used a Los Alamos-cast and -machined Composition B charge and a plane-wave detonation generator. An engineering test (CST-ENG) was conducted to test the charge response and permit necessary adjustments before the actual test. The charge for CST-ENG, 116.2 kg (256 lb), performed favorably according to the increased time-of-arrival data. However, the blast wave overpressure, 15.2 ± 1.4 MPa (2200 ± 200 psi), was higher than anticipated.

The charge for CST-9-RTG-5 was reduced to 93.1 kg (205 lb). After the test setup was verified, the charge was detonated and a blast wave of 15.3 ± 1.5 MPa (2212 ± 220 psi) overpressure and 16.6 ± 3.5 kPa · s (2.4 ± psi · s) impulse impacted the heated (1091 ± 10° C) module stack. The high overpressure was attributed to a change in the length-to-diameter ratio (L/D) of the charge, which modified the directed blast energy. The L/D of the cylindrical charge in CST-ENG was 0.49, whereas the charge L/D in CST-9-RTG-5 was 0.39. According to SNLA data, there is little variation in charge response of Composition C-4 explosives when the L/D is in the range of 0.4 to 0.6 for identical weight charges. We assumed that Composition B charges would follow the same guidelines.

The blast wave stripped the graphitics from the simulant-fueled clads. Clad M-46, from the blind end of the C-GIS (Fig. 67), was recovered in two pieces at a sawdust depth of 3.8 m. Most of this clad was recovered 0.76 m south of, and 0.70 m lower than, the original shock tube centerline. It contained approximately half of the simulant fuel. Particle size data of the retained fuel are shown in Table II. An iridium fragment identified as part of clad M-46 was recovered about 0.61 m north of the centerline. The larger portion containing the fuel appeared to have a downward trajectory as judged by its position in the sawdust.

A second clad, M-40 from the blind end of the A-GIS, was recovered integral at about 6.0 m deep and 0.4 m north of the original centerline (Fig. 68). The two remaining fueled clads were not recovered. The entire

shock tube was displaced about 0.5 m toward the catch tube and about 0.7 m north by the blast. We believe that the two missing clads, which had been on the north side of the module stack, had trajectories that missed the catch tube.

The iridium fragment from M-46 was examined to determine the probable cause of failure. Macroscopic examination revealed striations and cracks (Fig. 69) on the exterior surface, suggestive of collision with a large object or high-velocity metal fragment. Energy dispersive spectrometer (EDS) analysis of the fragment fracture surface at low magnification produced spectra indicating iridium and iron (Fig. 70). The specimen (Fig. 71a) was dot-mapped to clearly identify the iridium (Fig. 71b) and iron (Fig. 71c) areas. High-magnification EDS spectra (Fig. 72) of the same area (Fig. 73a) also indicated the presence of iridium and iron on the exterior surface. Dot mapping of the area shows the surface distribution of iridium (Fig. 73b) and iron (Fig. 73c). These results suggest that the clad collided with a steel object (either the shock tube or catch tube walls).

Clad M-40 was sectioned and the fuel simulant was sized. Particle size data are listed in Table II. Examination of a cratered section removed from the vent cup (Fig. 74) revealed significant grain elongation (Fig. 75). The crater penetrated approximately 35% of the capsule wall. The capsule weld had a typical microstructure, and both iridium cups were uniformly fine grained (Table III).

IV. DISCUSSION

The results of the postmortem examinations indicate a correlation between overpressure and fueled clad damage. Clad deformation (Table V) shows a tendency to increase as the overpressure increases. The overpressure, acting through an RTG housing, strips the graphite away from the fueled clads at a minimum overpressure between 2.96 MPa (429 psi) and 5.1 MPa (736 psi), leaving only bare capsules to resist subsequent impacts. Without the intervening housing, the graphite is stripped away at an overpressure between 5.1 MPa (735 psi) and 7.4 MPa (1070 psi).

The RTG housing does not act as a protective shield for the GPHS modules as was originally assumed in prior RTG design and test programs. The first CST, conducted at the same blast parameters as BMT-2, showed a marked increase in damage to the GPHS module. The intervening RTG housing apparently acts as a flyer-plate-type fragment. The housing fragment sizes are inversely proportional to the overpressure.

None of the fueled clads appeared to be breached by the overpressure alone. All of the breached clads (in CST-5-RTG-1, CST-7-RTG-3, and CST-9-RTG-5) apparently collided with high-density fragments. The breached fueled clad in CST-5-RTG-1 may have been hit by a stainless steel weight segment from the GE RTG simulant, and clads in CST-7-RTG-3 and CST-9-RTG-5 apparently breached as a result of collision with the shock tube or catch tube walls.

Surface cratering on the fueled clads does not appear to be directly related to the overpressure exposure. Electron microprobe analysis of a typical crater in the CST-7-RTG-3 clad indicated that a possible cause of the crater was dirt, which was probably propelled down the shock tube with the blast wave.

The explosion overpressure hydrostatically compresses the clad around the fuel, reducing or eliminating the gaps between components. This effect becomes more pronounced as the overpressure increases.

All of the iridium cups had fine-grained microstructures (Table III). The average grain sizes ranged from 21.9 to 31.7 grains/0.635-mm nominal wall thickness. Although the test temperatures varied slightly, from 1080°C to 1110°C, the performance of the iridium cups used in the overpressure test series should be considered representative of flight-quality clad response.

V. CONCLUSIONS

On the basis of the test results described above, we conclude the following about the response of the GPHS to pressures generated in shock tubes by high explosives:

(1) The static pressure required to strip the graphite components from the fueled clads of a bare module is between 5.1 MPa (735 psi) and 7.4 MPa (1070 psi).

(2) The static pressure required to strip the graphite components from fueled clads with an intervening RTG simulant is between 2.96 MPa (429 psi) and 5.1 MPa (736 psi).

(3) Overpressures of up to 15.2 $\pm$ 1.5 MPa (2200 $\pm$ 220 psi) alone do not appear to result in a fuel release; subsequent collision with a high-density fragment or impact against an unyielding surface is necessary to breach the clad.

(4) Clad deformation (M/m) and fuel fragmentation increase with overpressure magnitude.

(5) Fueled clad deformation appears to be independent of location within the module.

VI. RECOMMENDATIONS

It is important for the overall safety analysis of the GPHS to determine the actual overpressure at which only the aeroshell is removed and that at which the GIS is also removed. Accordingly, we recommend additional testing to determine

(1) The overpressure threshold at which the aeroshell is removed while still leaving the impact shells intact;

(2) The overpressure threshold at which the impact shells are removed from the clads.

ACKNOWLEDGMENTS

We thank the following people for their valuable assistance in completing these tests: C. M. Seabourn for his supervision of the bare module tests; L. Berg, F. Mathews, B. Berg, and other SNLA personnel for test range operations and shock wave diagnostics; A. Herrera, M. Anstey, W. Hults, and R. E. Tate for test assembly and posttest recovery; J. Archuleta for metallography and SEM analyses; D. Garinger for particle size analyses; J. Lucero and H. Gasca for x-ray support; C. Baca, D. Court, and F. Martinez for design and assembly support; and L. Vaughn for graphite outgassing.

REFERENCES

1. "Space Shuttle Data for Planetary Mission Radioisotope Thermoelectric Generator (RTG) Safety Analysis," National Aeronautics and Space Administration document JSC 08116 (February 1985).

2. A. B. Willoughby, C. Wilton, and J. Mansfield, "Liquid Propellant Explosive Hazards," URS Corporation document AFRPL-TR-68-92 (December 1968).

3. "GPHS Safety Verification Test Series Procedures Manual," Los Alamos National Laboratory document MST-5-C-83-19 (April 14, 1983).

4. "GPHS-RTG System Explosion Test. DIRECT COURSE Experiment 5000," Advanced Energy Programs Department, General Electric Company document GESP-7181 (March 1984).

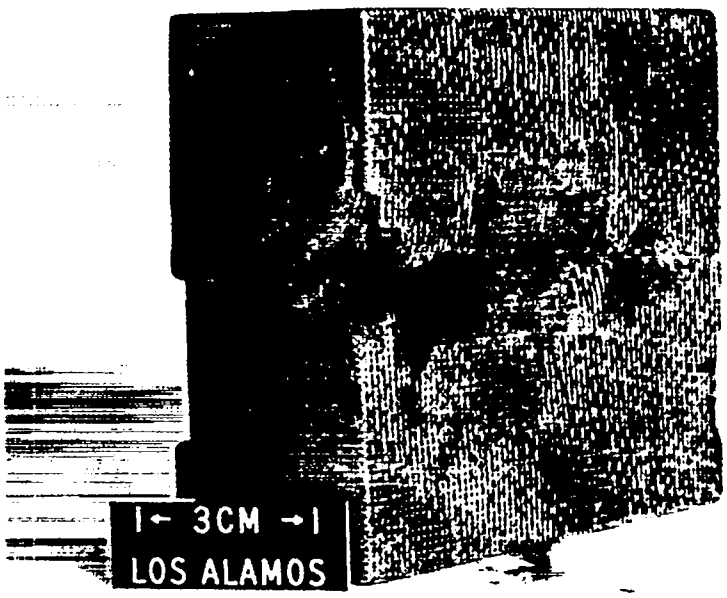

Fig. 8. After the sequential 1.4- and 5.1-MPa overpressure tests, the GPHS aeroshell was fractured. The blast impacted the narrow surface of the GPHS module facing up in the figure.

Fig. 9. The C-GIS containing capsules IRG-117 and IRG-118 was broken after the 5.1-MPa blast. Simulant-fueled clad IRG-118 is visible.

Fig. 10. The A-GIS containing simulant-fueled clad IRG-115 and IRG-116 appeared undamaged after the 5.1-MPa blast. The A-GIS was on the blast side of the module.

IRG-115

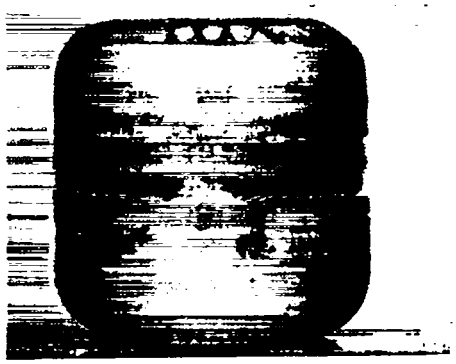

IRG-116

IRG-117

IRG-118

Fig. 11. Simulant-fueled clads after sequential overpressure tests at 1.4 and 5.1 MPa.

Fig. 12. The simulant fuel (UO_2) in clad IRG-118 was broken into relatively large fragments after the two sequential explosion tests.

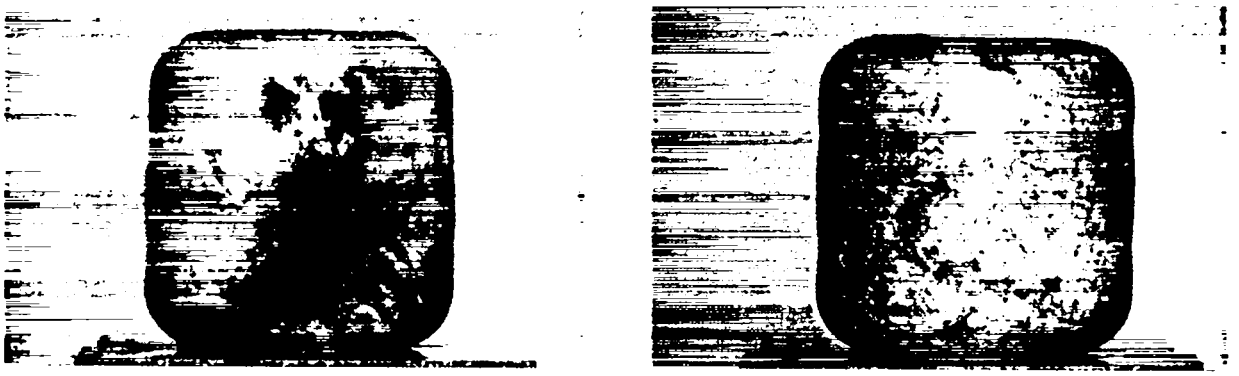

Capsule A Capsule B

Fig. 13. Simulant-fueled clads after overpressure test at 7.4 MPa. Capsule D penetrated the plywood bulkhead at the end of the catch tube.

Capsule C

Capsule D

Fig. 13. (cont)

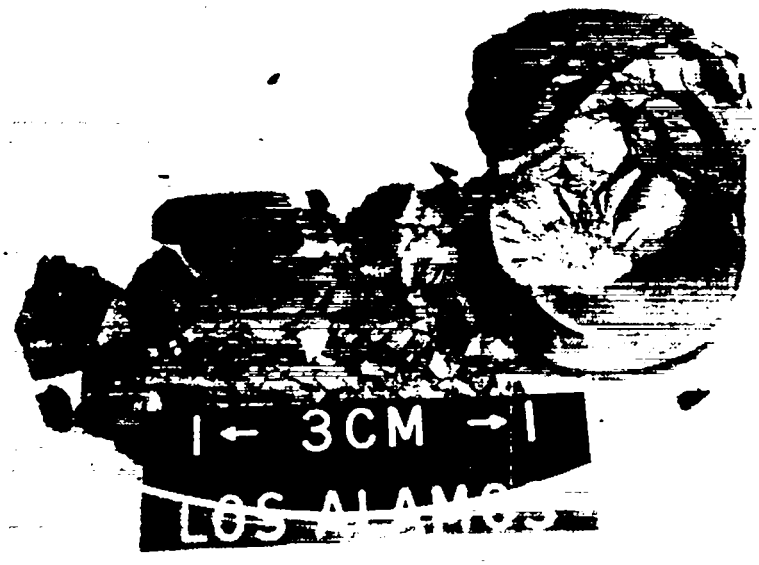

Fig. 14. One end of the UO_2 pellet from capsule C in BMT-3 was fragmented; 1.5X.

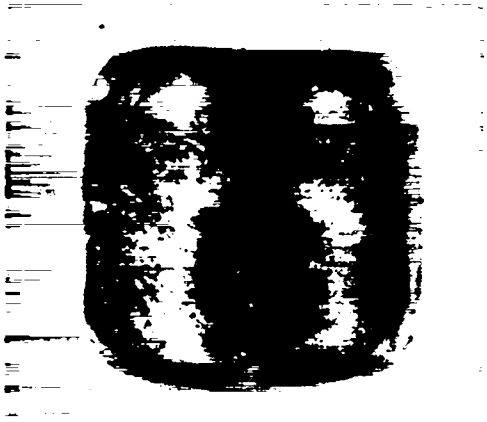

Clad 1

Clad 2

Clad 3

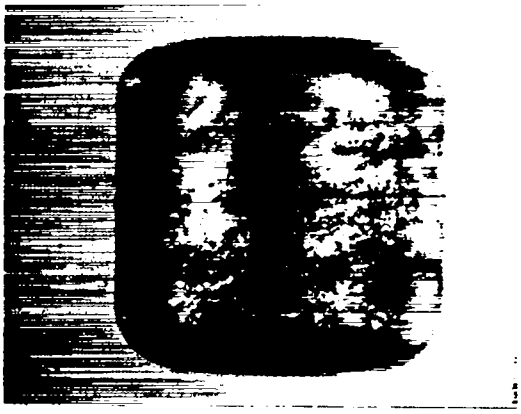

Clad 4

Fig. 15. Simulant-fueled clads after CST-1 at 5.1-MPa overpressure.

Fig. 16. A deep crater was observed on the CST-1 clad selected for examination; 10.5X.

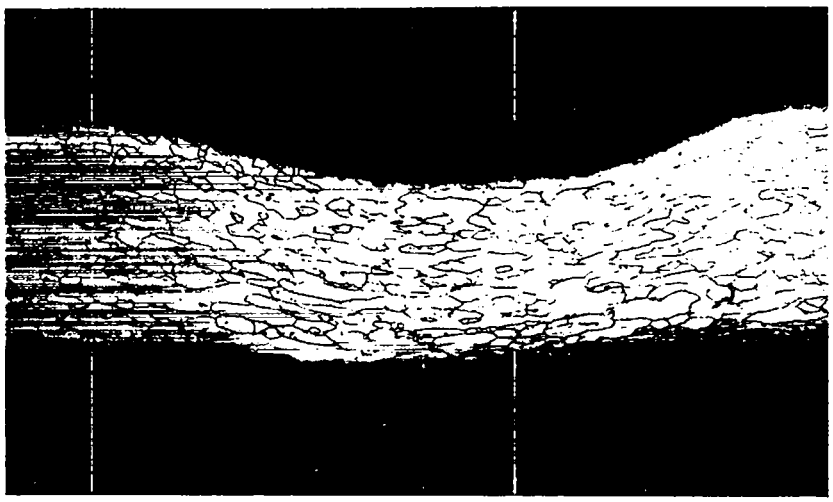

Fig. 17. The iridium grains were elongated in the Clad 1 cratered area; etched, 50X.

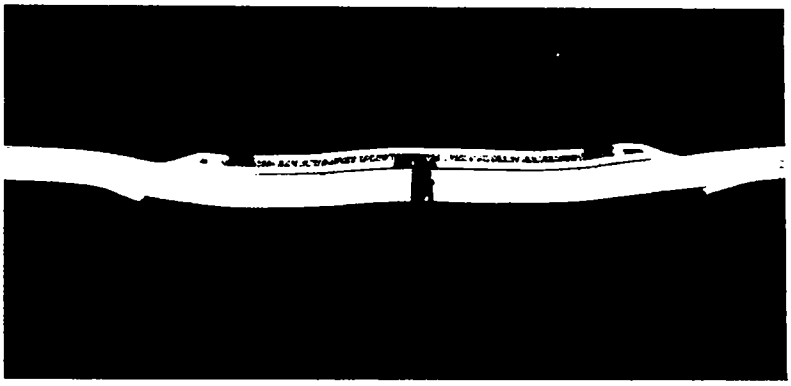

Fig. 18. The CST-1 capsule vent was undeformed; as polished, 7X.

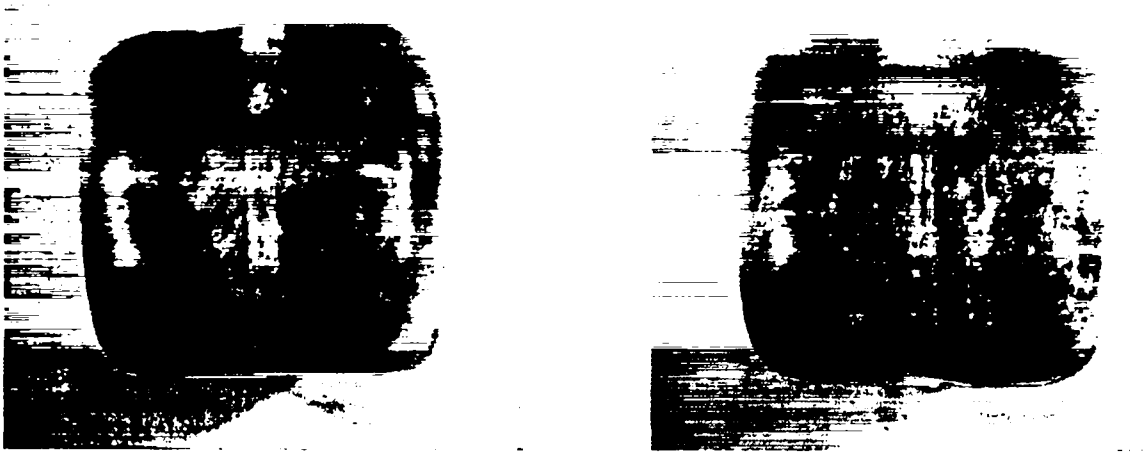

IRG-125 IRG-126

Fig. 19. Simulant-fueled clads after CST-2 at 7.1-MPa overpressure.

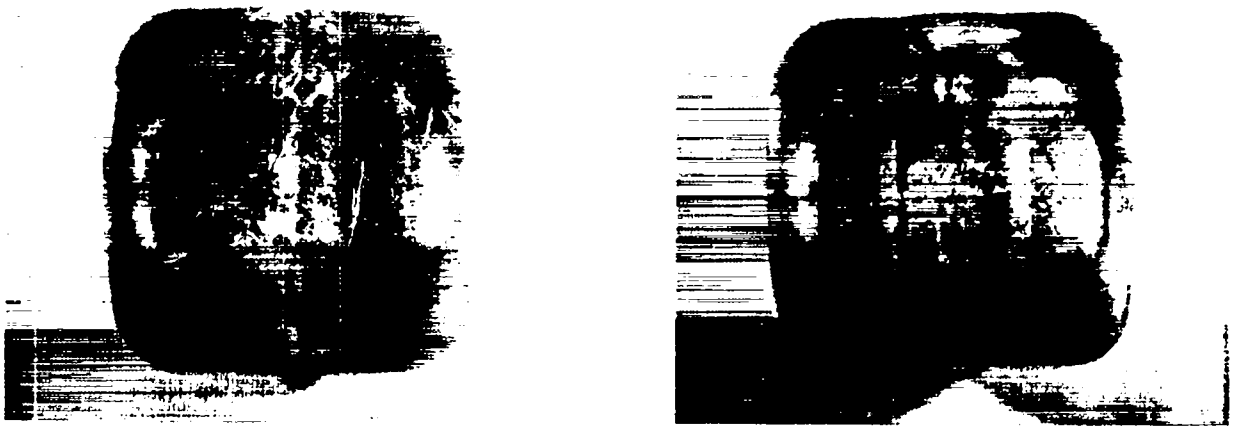

IRG-127 IRG-128

Fig. 19. (cont)

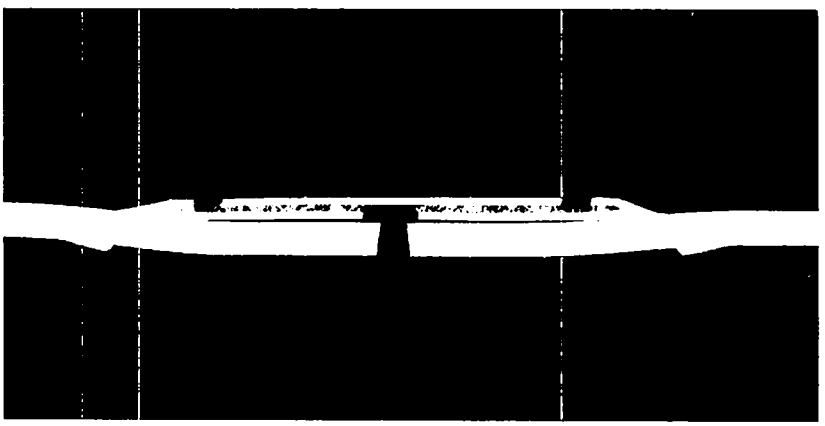

Fig. 20. The CST-2 capsule vent was undeformed and contained no mechanical defects; as polished, 7X.

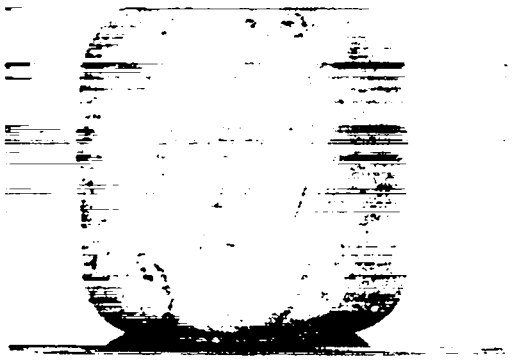

L-12

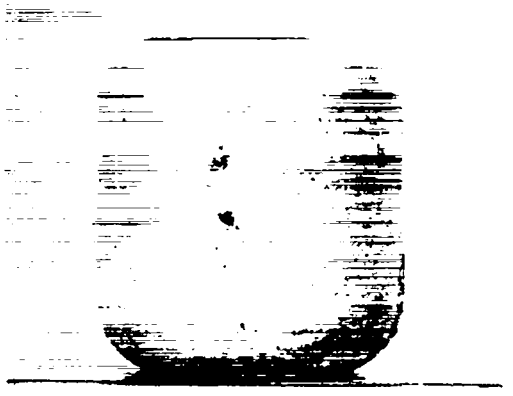

L-14

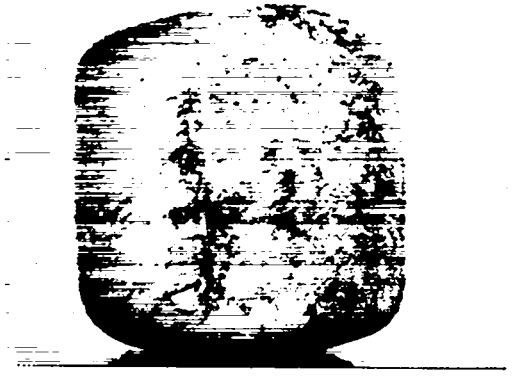

L-16

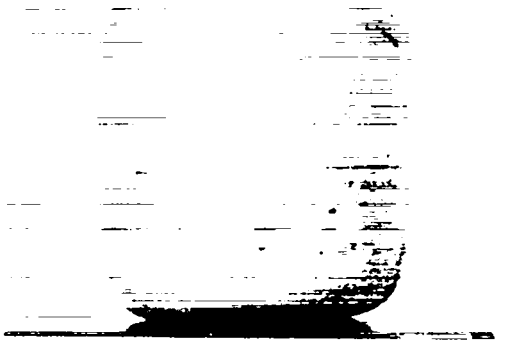

L-19

Fig. 21. Simulant-fueled clads after CST-3 at 11.6-MPa overpressure.

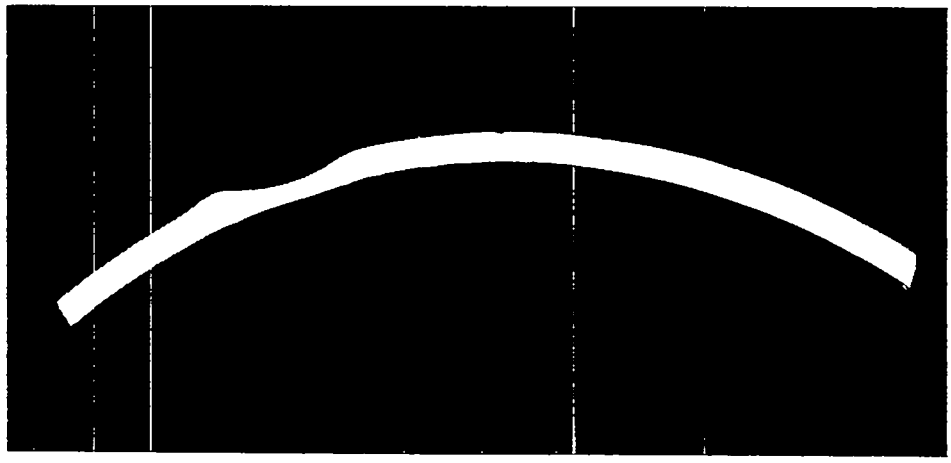

Fig. 22. The crater on the L-12 weld shield cup penetrated 38% of the wall thickness; as polished, 7X.

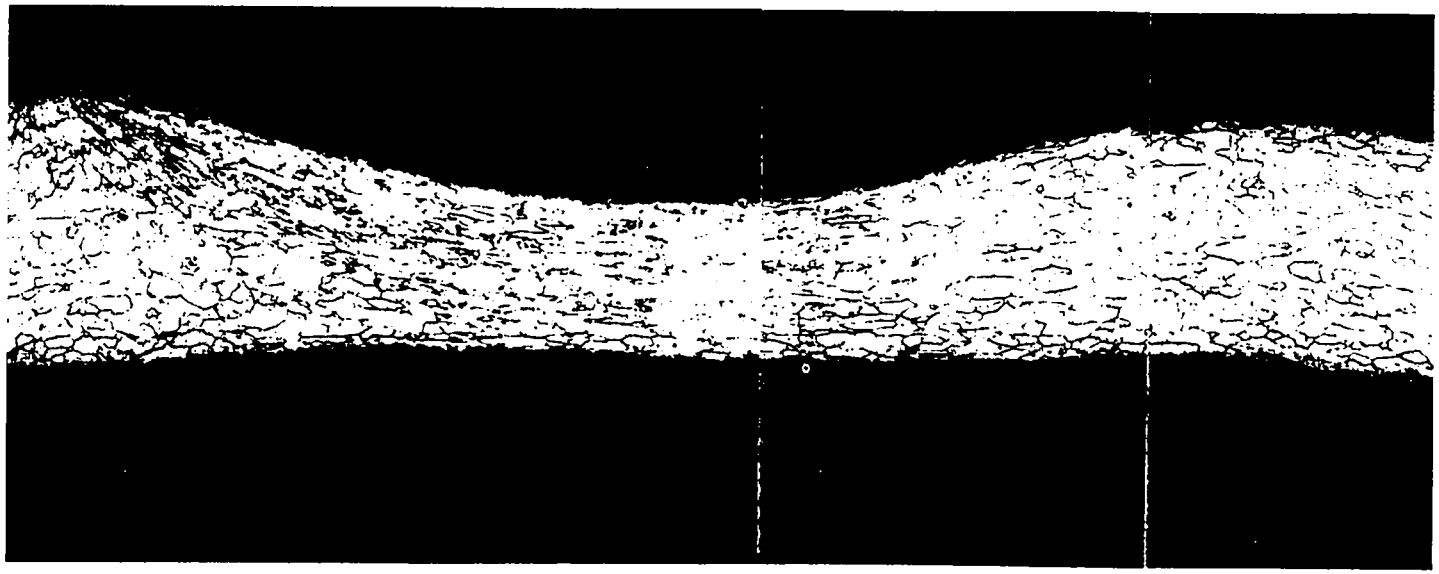

Fig. 23. The L-12 capsule wall within the crater displayed significant ductility; etched, 50X.

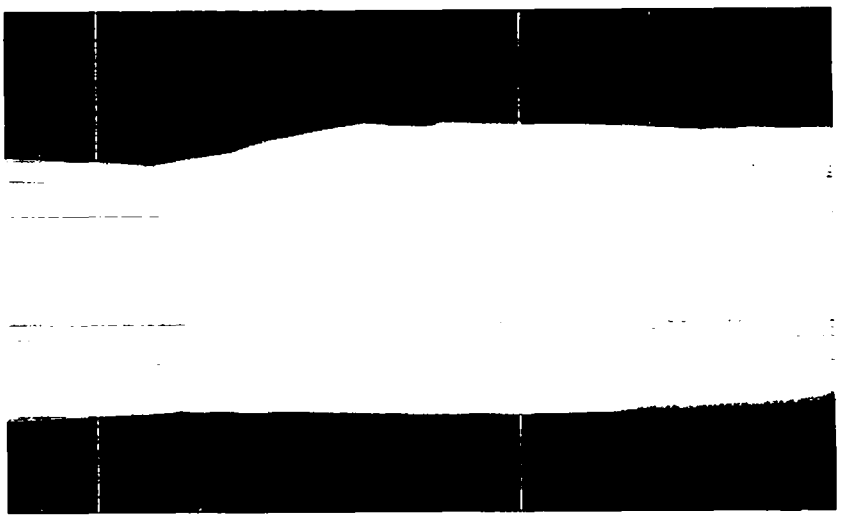

(a)

(b)

Fig. 24. The L-12 closure weld had a very unusual microstructure. (a) As polished and (b) etched; both at 50X.

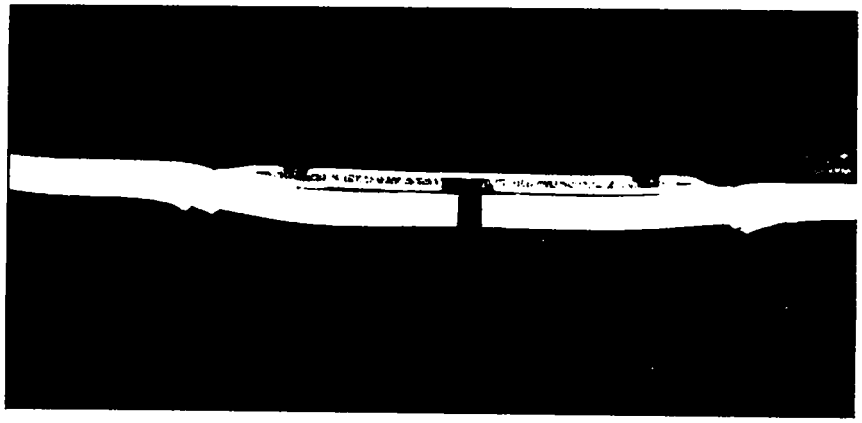

Fig. 25. The L-12 capsule vent was undeformed; as polished, 7X.

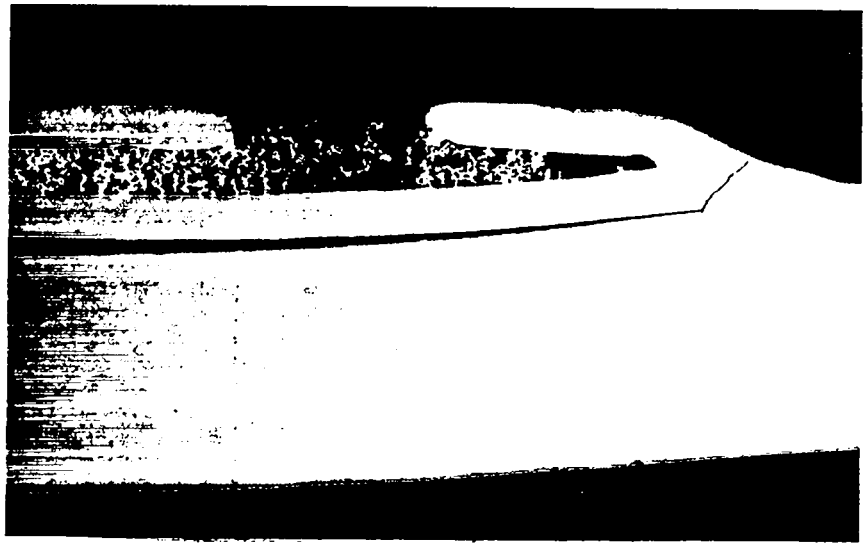

Fig. 26. A small crack was observed on one side of the L-12 vent assembly; as polished, 50X.

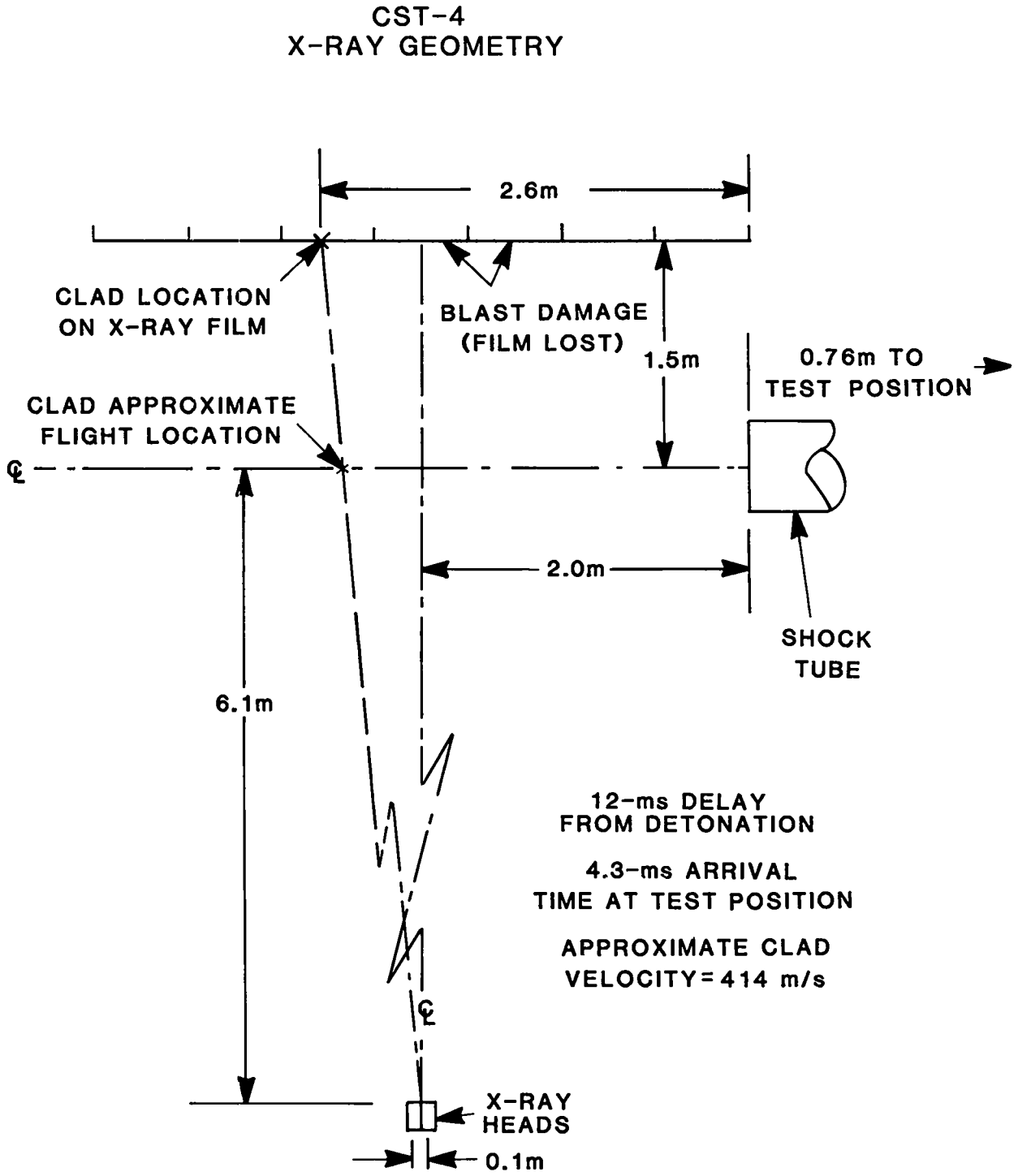

Fig. 27. The CST-4 simulant clad traveled 3.2 m in 7.7 ms (assuming it was traveling on the shock tube centerline).

L-9

L-10

L-15

L-23

Fig. 28. The simulant-fueled clads after CST-4 at 12.2 MPa overpressure.

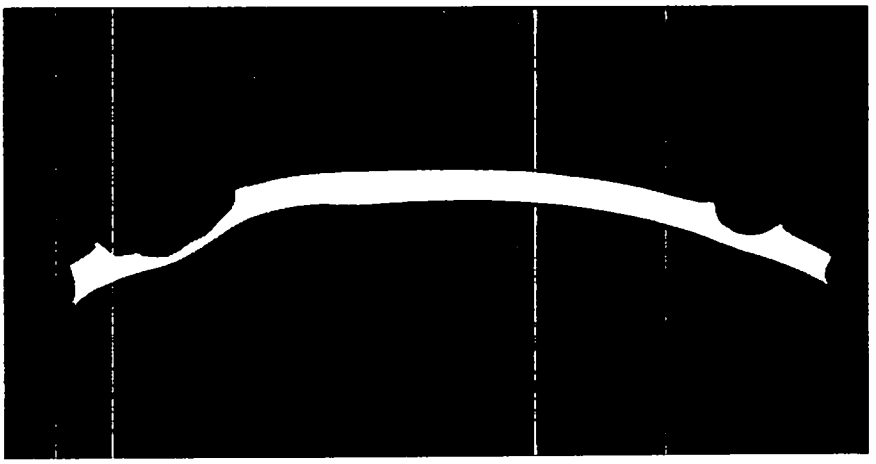

Fig. 29. A transverse section containing the large crater and a smaller indentation was removed from the L-10 weld shield cup; as polished, 7X.

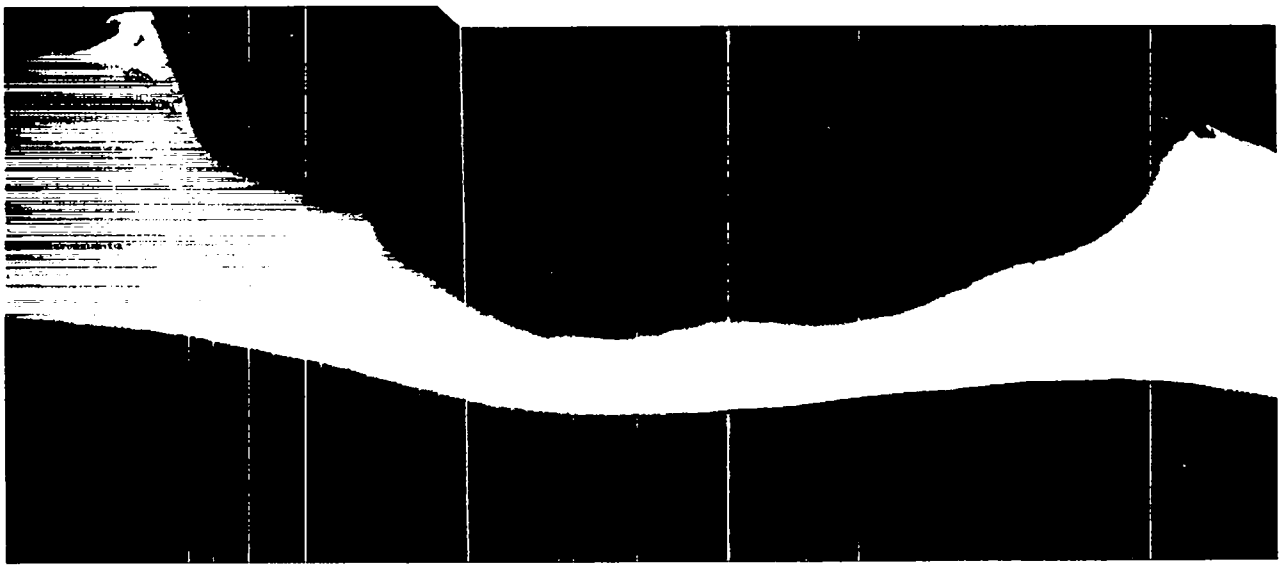

Fig. 30. The large crater penetrated more than 70% of the L-10 capsule wall; as polished, 50X.

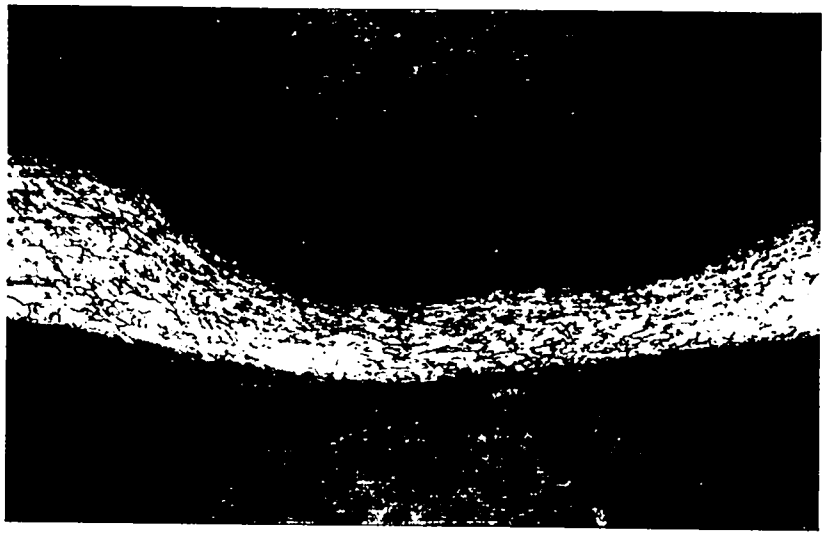

(a)

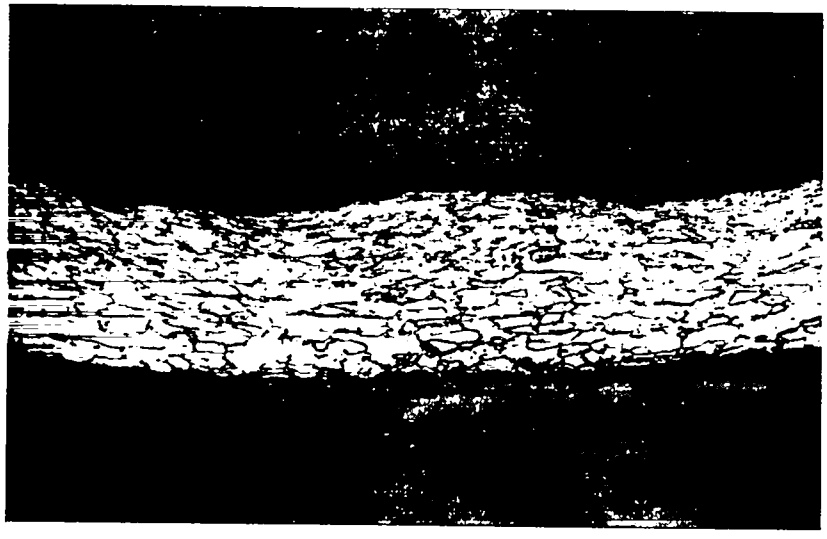

(b)

Fig. 31. The capsule wall within the crater was severely deformed. (a) Etched, 50X; (b) etched, 100X.

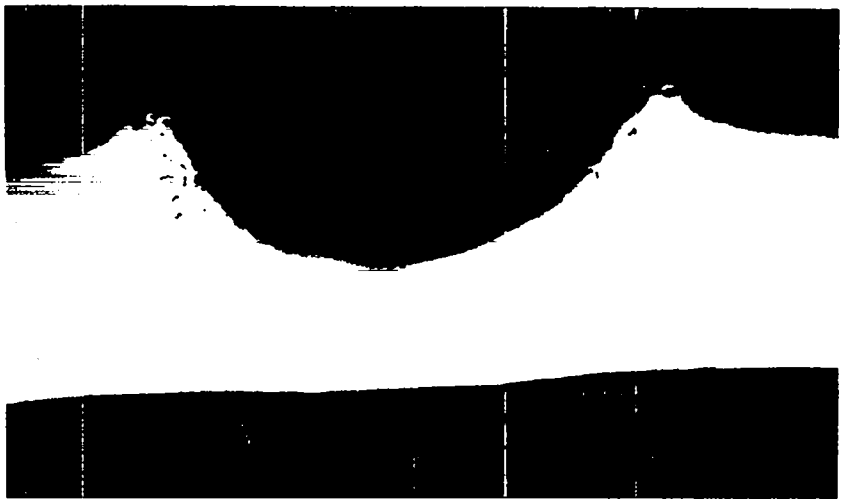

(a)

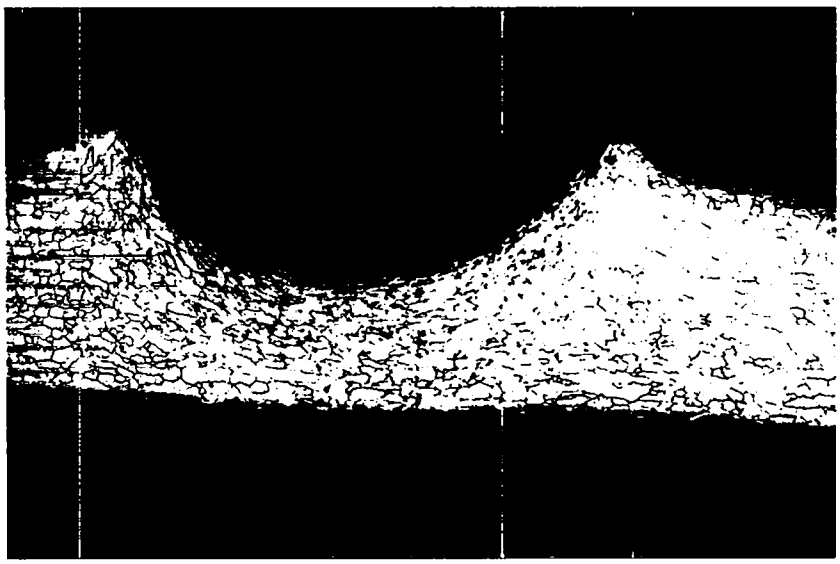

(b)

Fig. 32. The small indentation was similar to the large crater. (a) As polished and (b) etched; both at 50X.

Fig. 33. A crater in the L-10 vent cup penetrated 40% of the wall thickness; as polished, 7X.

(a)

Fig. 34. The large crater in the vent cup of clad L-10 produced a pattern of internal grain boundary cracks. (a) As polished and (b) etched; both at 50X.

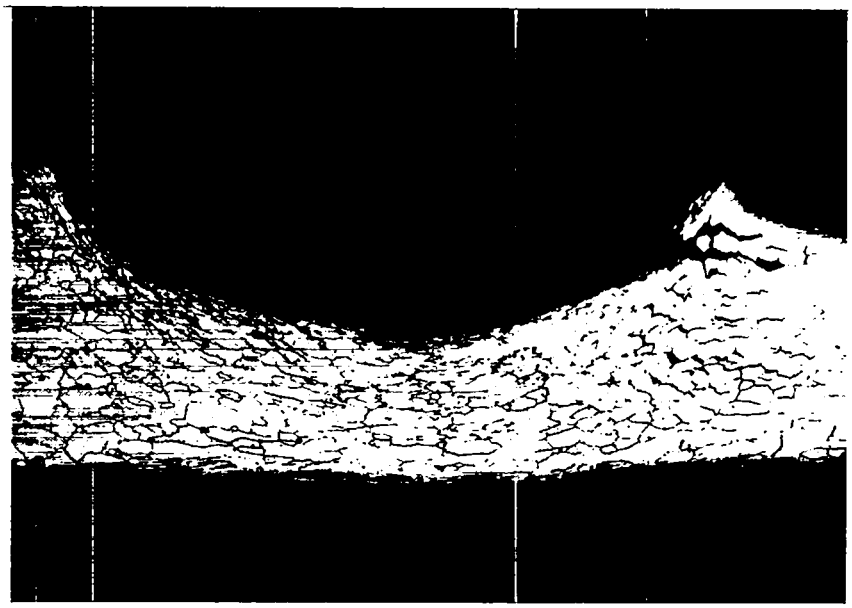

(b)

Fig. 34. (cont)

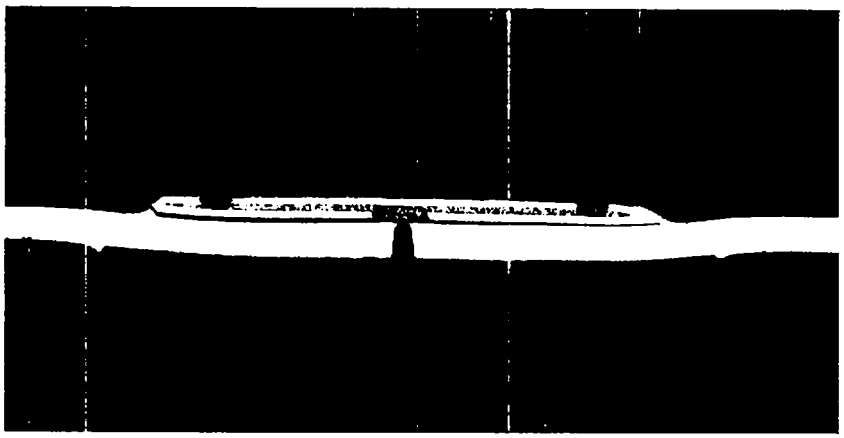

Fig. 35. The L-10 vent was not deformed; as polished, 7X.

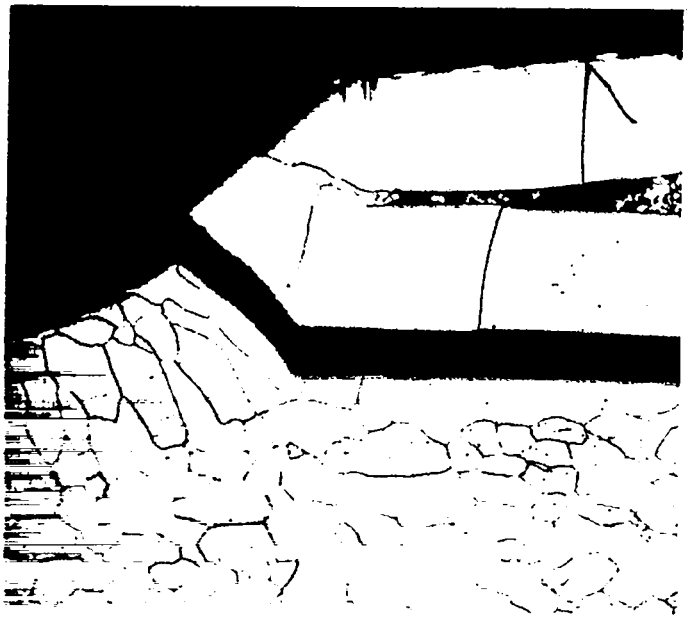

(a)

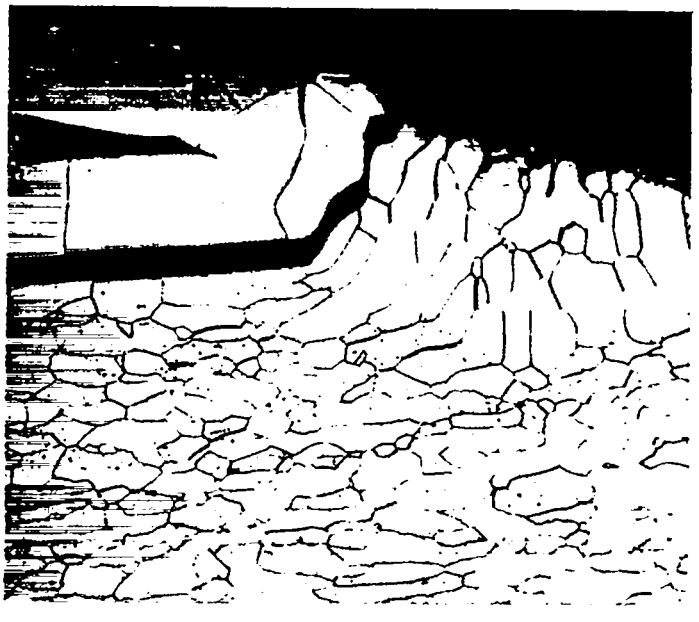

(b)

Fig. 36. Both sides (a, b) of the L-10 vent assembly were cracked; etched, 50X.

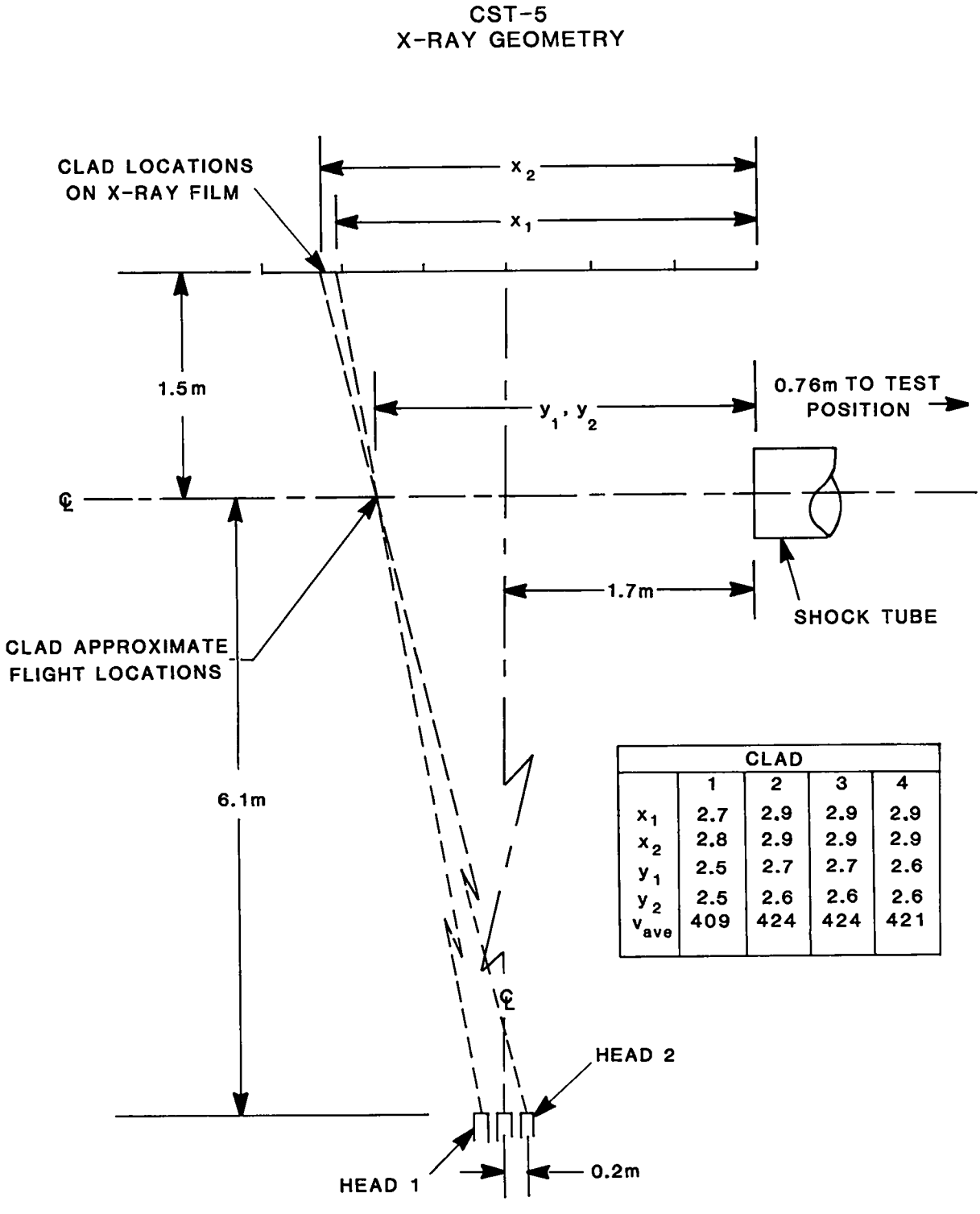

	CLAD			
	1	2	3	4
x_1	2.7	2.9	2.9	2.9
x_2	2.8	2.9	2.9	2.9
y_1	2.5	2.7	2.7	2.6
y_2	2.5	2.6	2.6	2.6
v_{ave}	409	424	424	421

Fig. 37. All four simulant clads were imaged intact on the x-ray films at approximately 3.4 m (assuming they were traveling on the shock tube centerline). A travel time of 8.057 ms was required to reach this position.

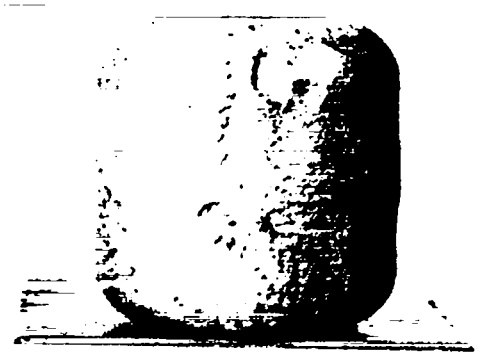

L-17

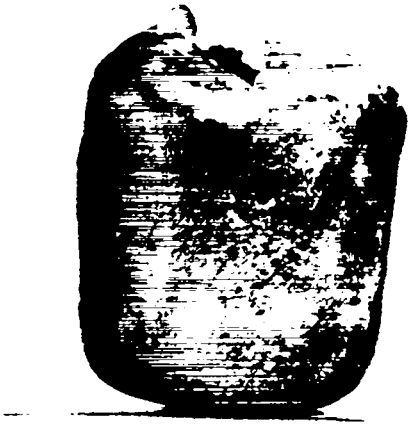

L-18

L-22

L-24

Fig. 38. The simulant-fueled clads after CST-5-RTG-1 at 12.5 MPa. Clad L-18 was breached by a stainless steel weight segment from the cylindrical RTG simulant.

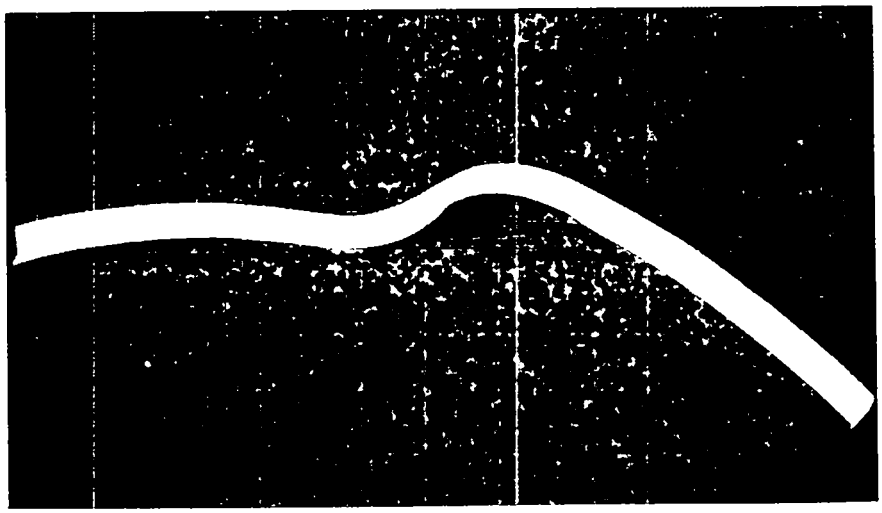

Fig. 39. Deep surface gouging was observed in a severely deformed section of the L-24 shield cup; as polished, 7X.

(a)

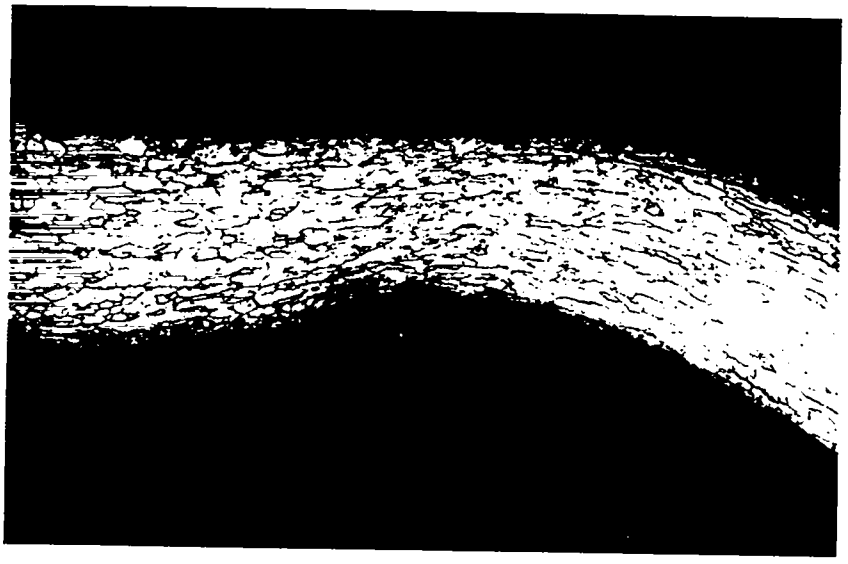

(b)

Fig. 40. Grain elongation was also observed in the shield cup section. (a) As polished and (b) etched; both at 50X.

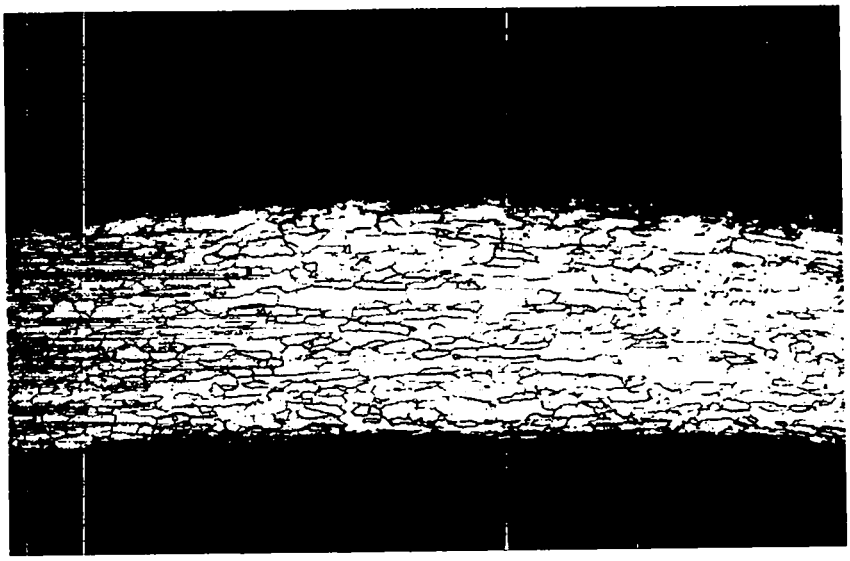

Fig. 41. Significant grain elongation was also observed in a deformed section of the L-24 vent cup; etched, 50X.

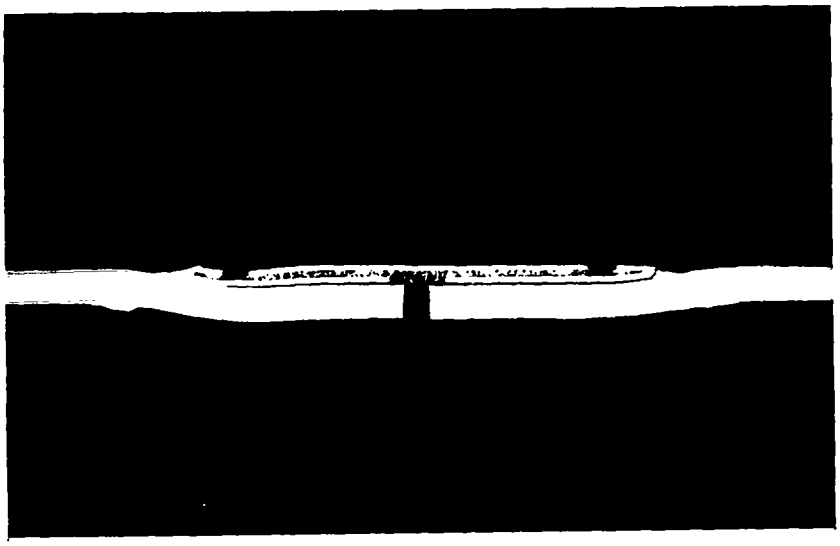

Fig. 42. The L-24 capsule vent was not significantly deformed; as polished, 7X.

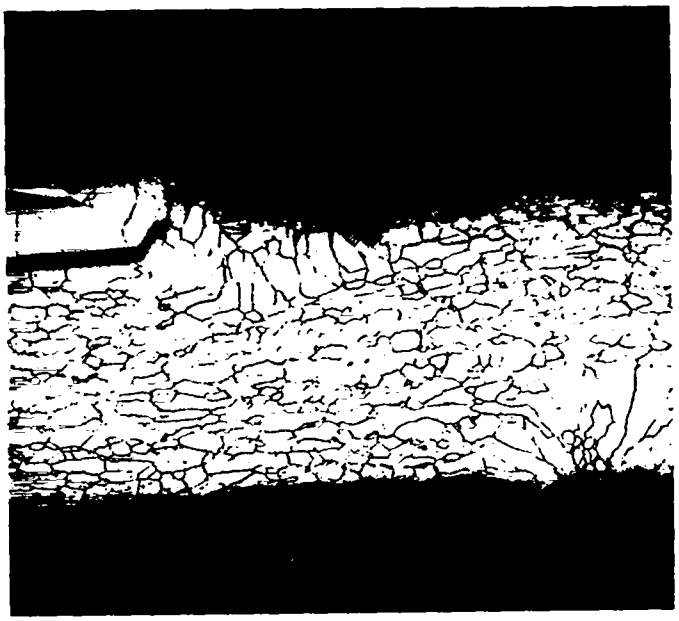

Fig. 43. One side of the L-24 vent assembly weld was cracked; etched, 50X.

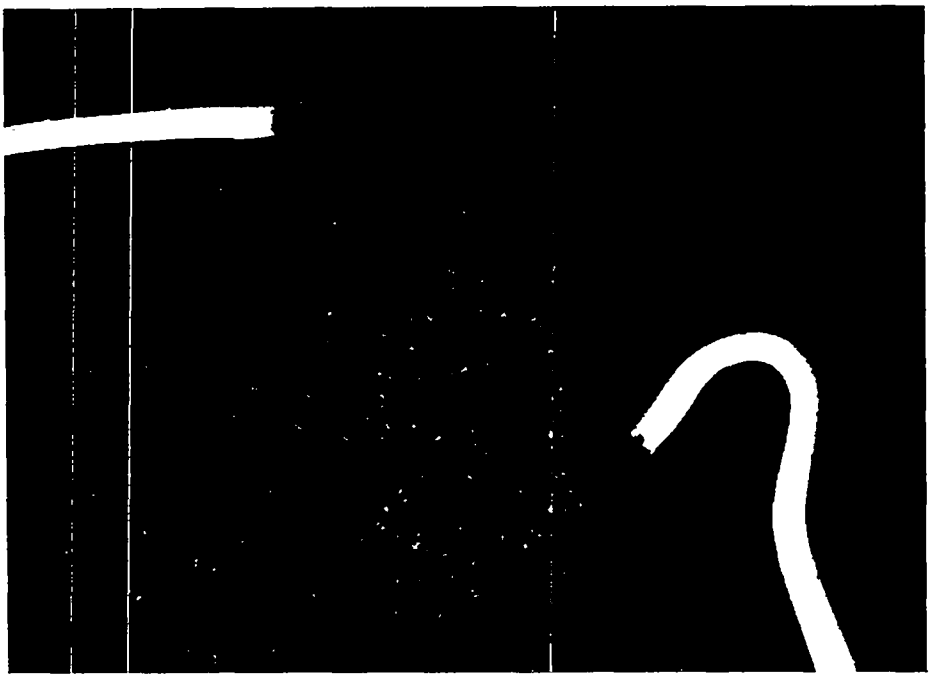

Fig. 44. A cross section of the L-18 breach was metallographically examined; as polished, 7X.

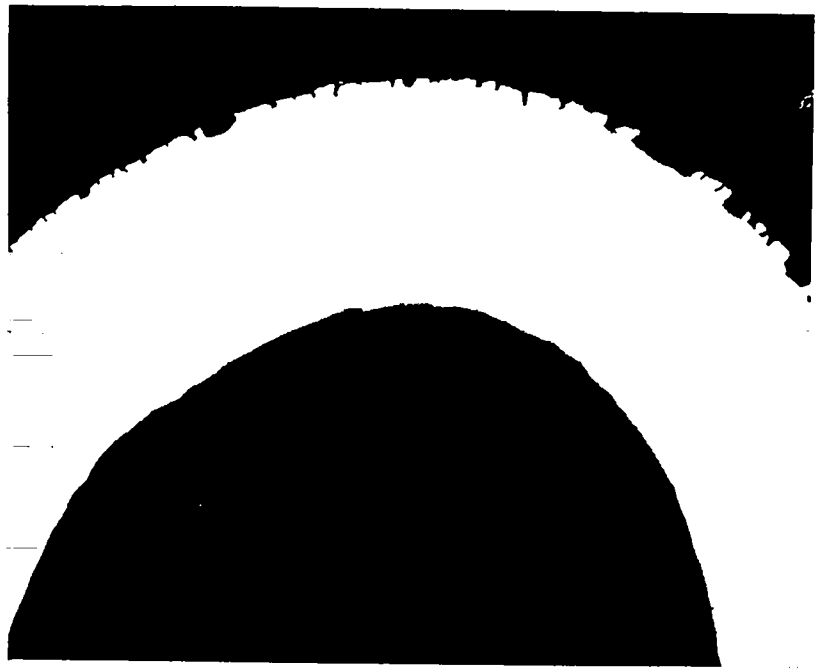

(a)

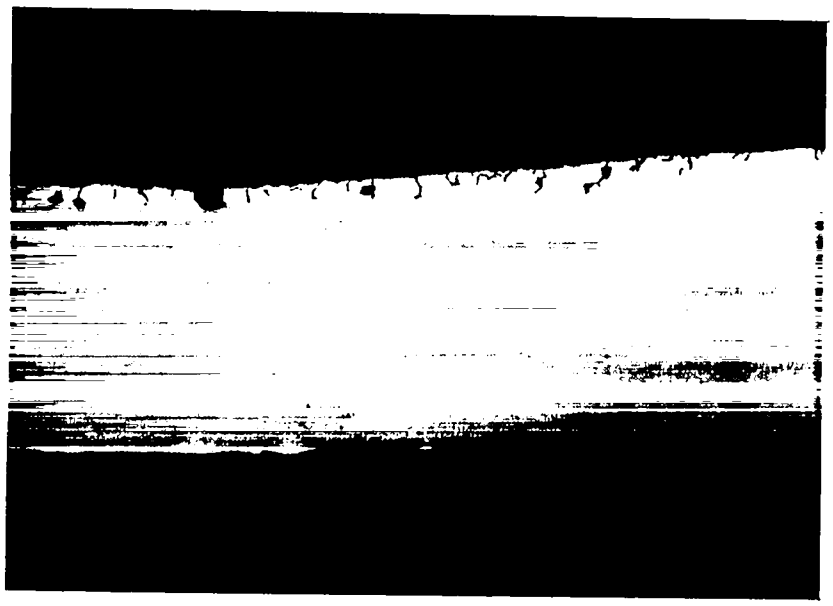

(b)

Fig. 45. One side of the L-18 breach was deeply gouged and cracked; two views (a, b), as polished, 50X.

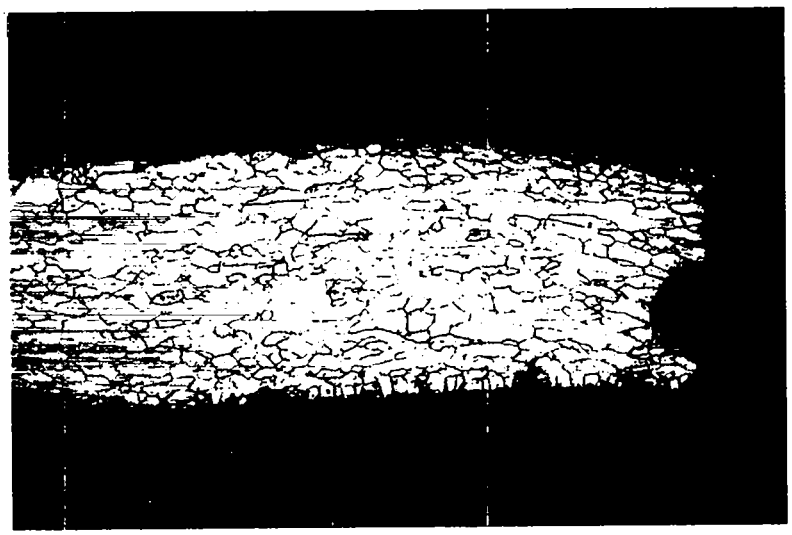

(a)

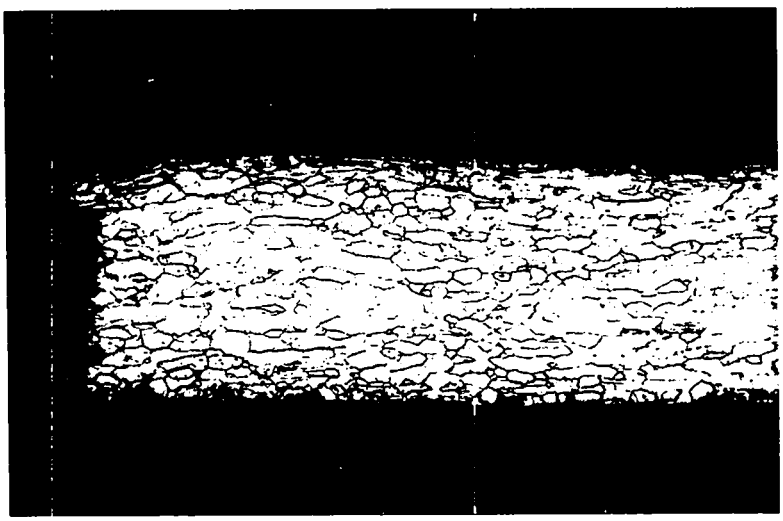

(b)

Fig. 46. Both sides (a, b) of the L-18 breach had a brittle, intergranular appearance; etched, 50X.

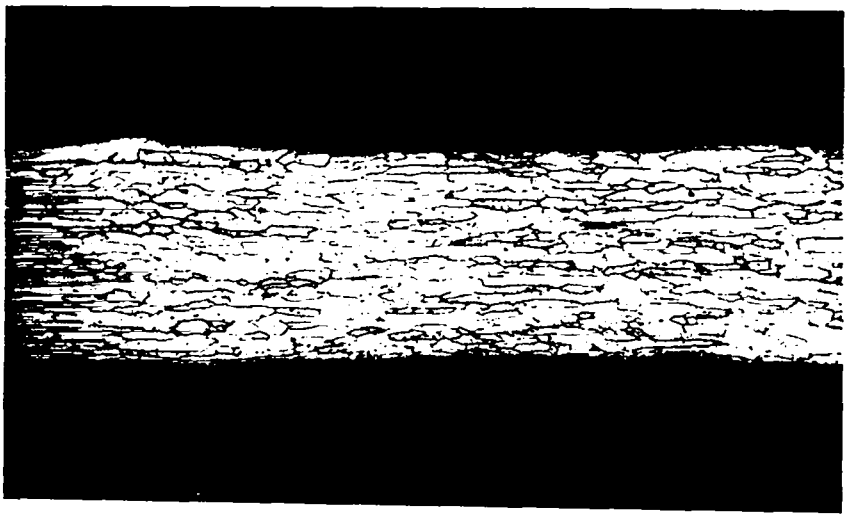

(a)

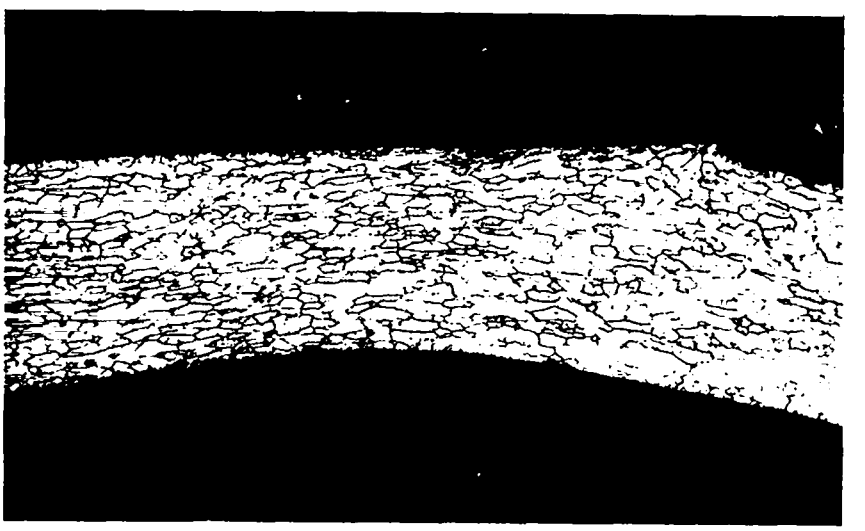

(b)

Fig. 47. Significant grain elongation occurred in some areas of the L-18 weld shield cup; two views (a, b), etched, 50X.

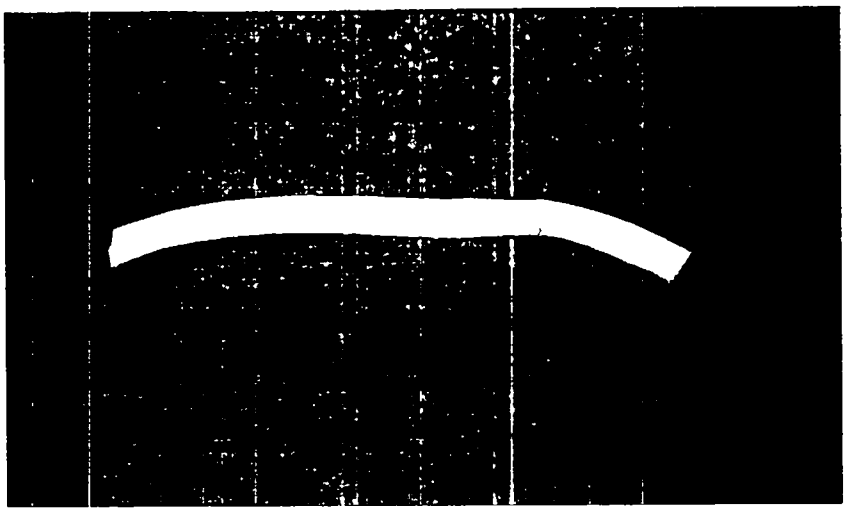

(a)

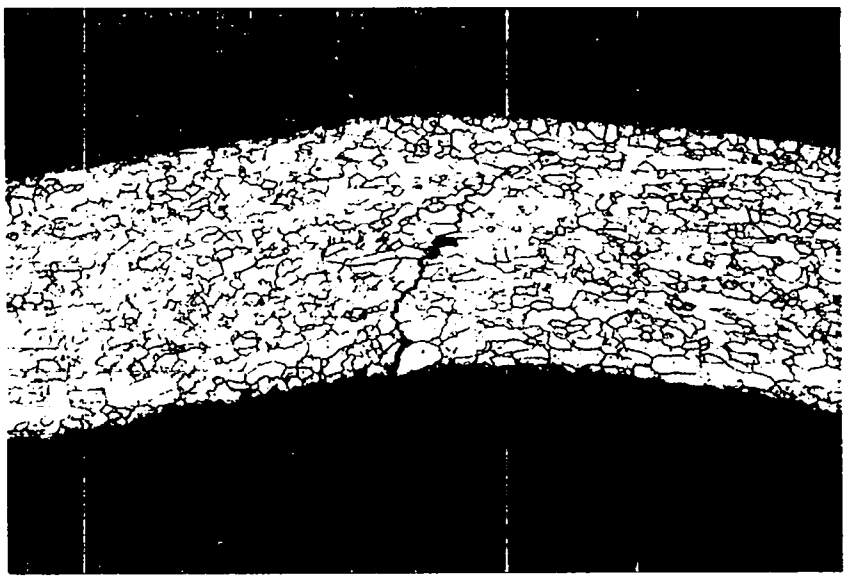

(b)

Fig. 48. A section of the L-18 vent cup contained a deep crack that penetrated 80% of the capsule wall. (a) As polished, 7X, and (b) etched, 50X.

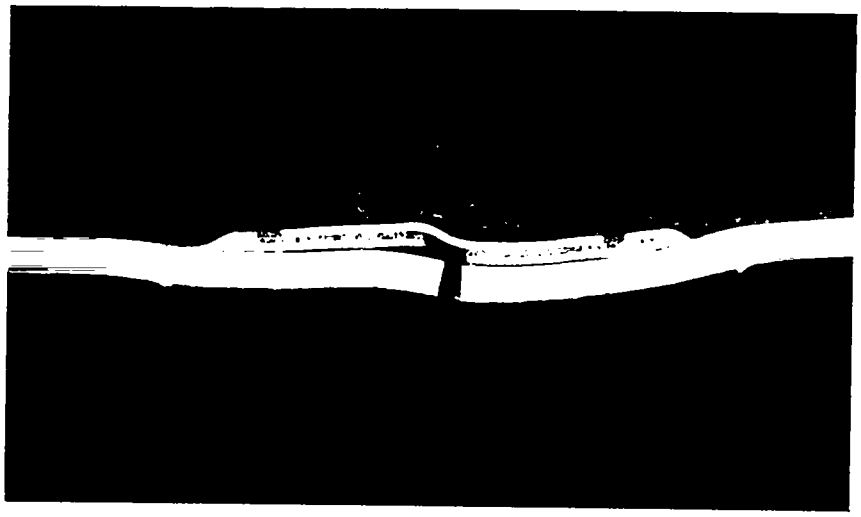

Fig. 49. The L-18 vent was severely deformed; as polished, 7X.

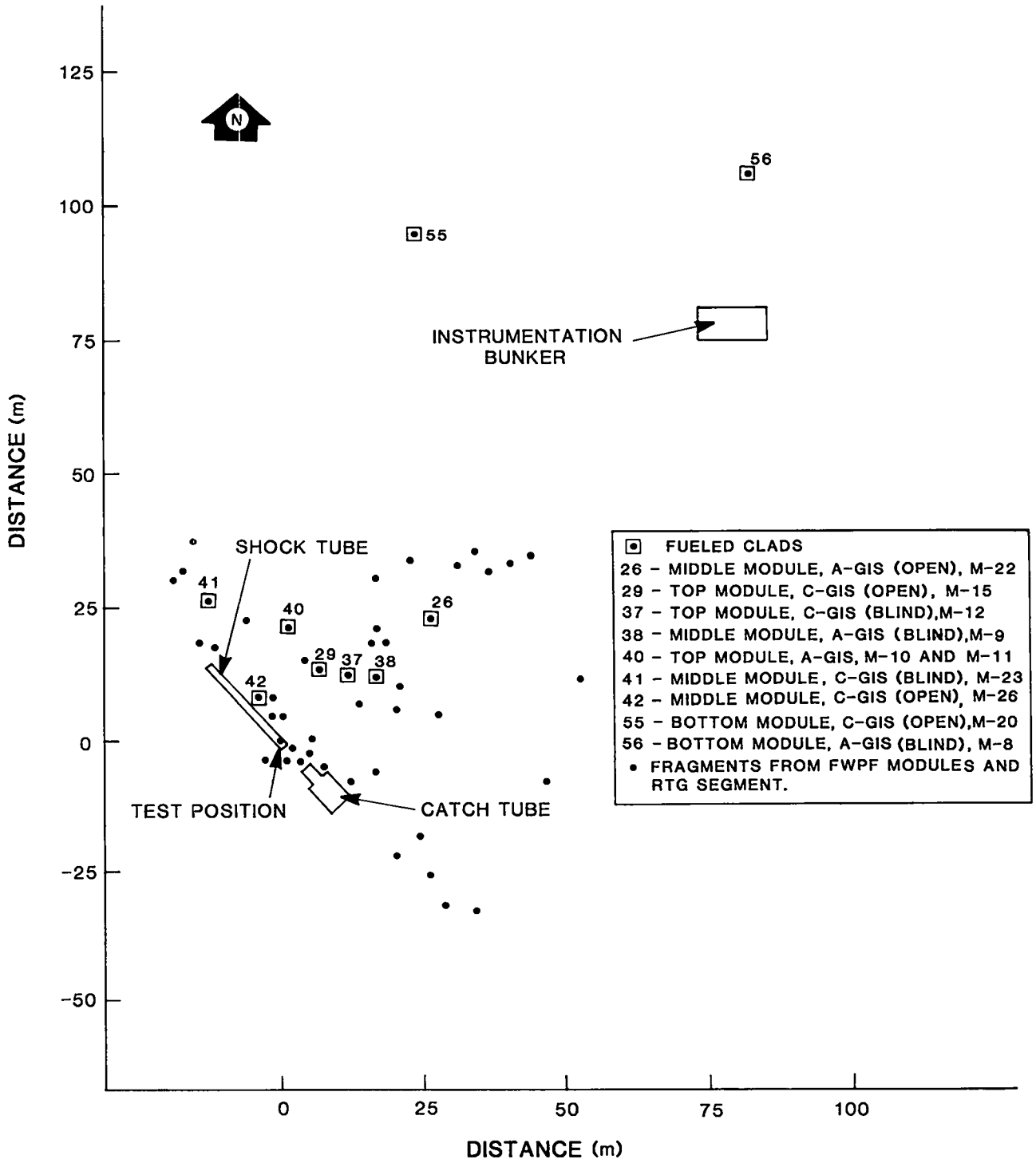

Fig. 50. The module test stack in CST-6-RTG-2, propelled upward by a reflected component of the blast wave, was scattered over a wide area.

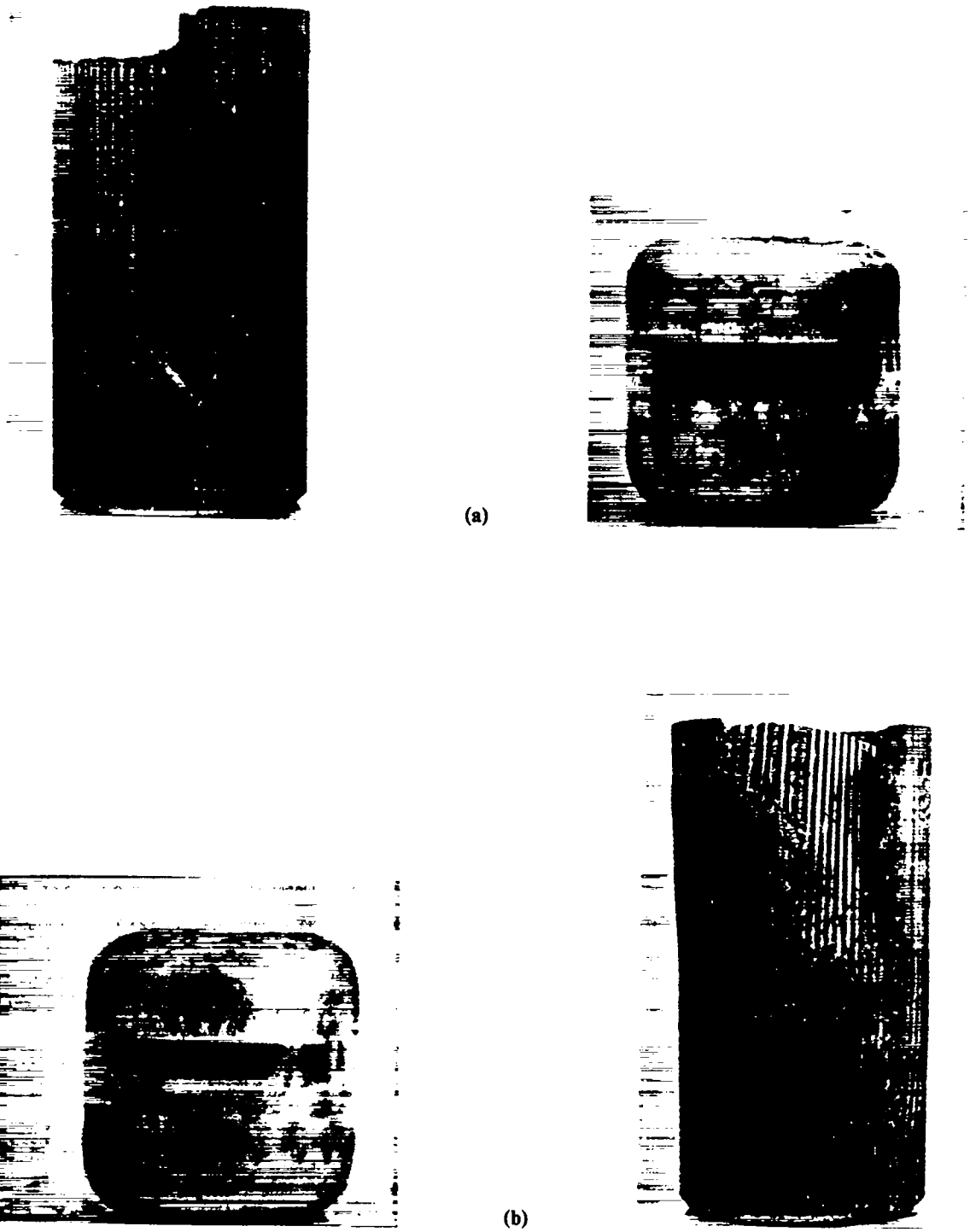

Fig. 51. (a) Clad M-12 (top module, C-GIS) and (b) clad M-9 (middle module, A-GIS) were recovered integral in their graphite impact shells. (c) Clads M-10 and M-11 (top module, A-GIS) were also recovered integral in the GIS.

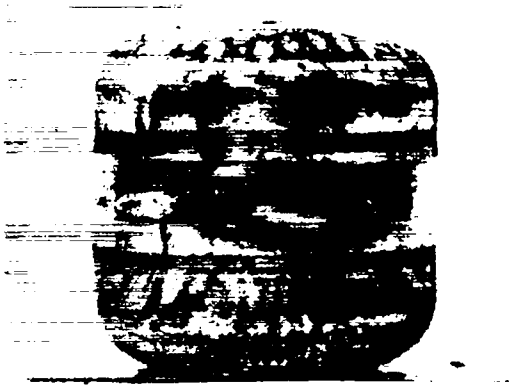

M-11

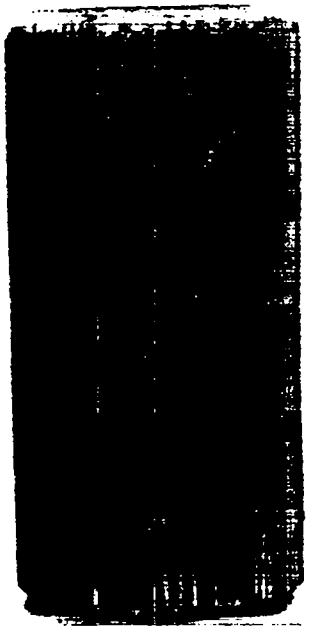

M-10

(c)

Fig. 51. (cont)

(a)

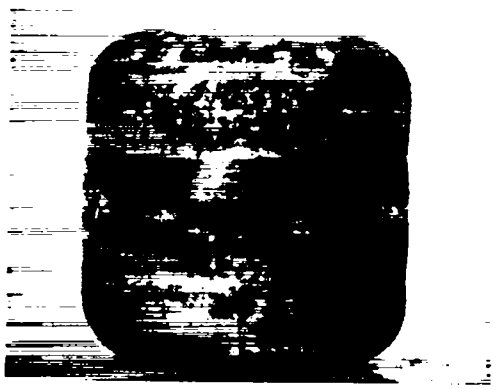

(b)

Fig. 52. Three bare clads were recovered integral: (a) M-26 (middle module, C-GIS); (b) M-15 (top module, C-GIS); and (c) M-23 (middle module, C-GIS).

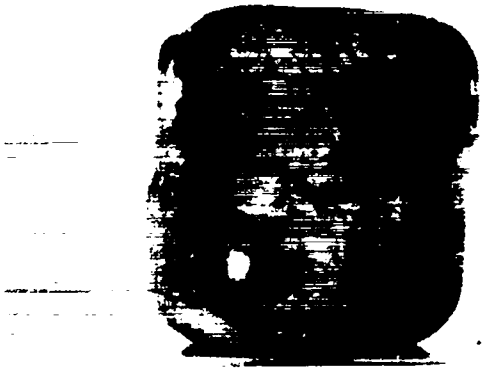

(c)

Fig. 52. (cont)

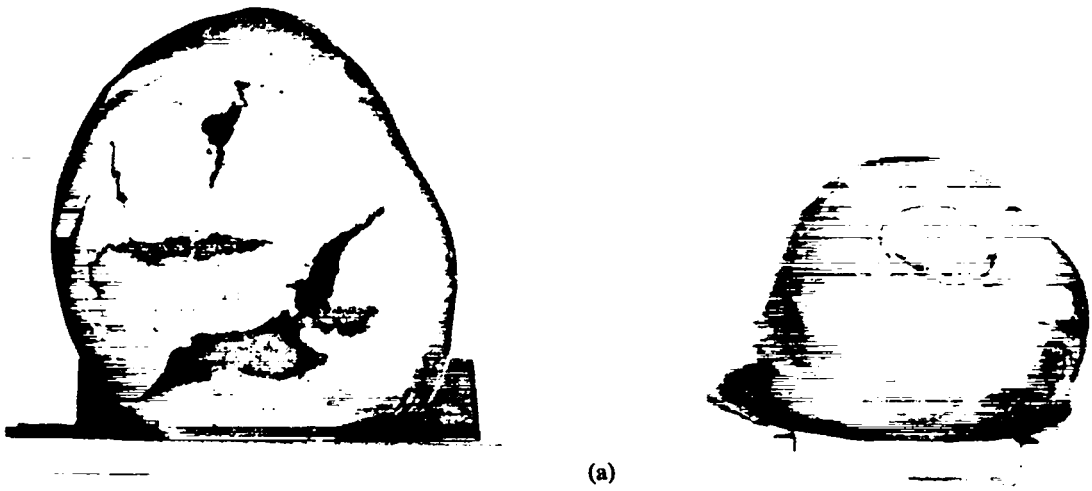

(a)

(b)

Fig. 53. Three clads were recovered breached: (a) M-8 (bottom module, A-GIS); (b) M-20 (bottom module, C-GIS); and (c) M-22 (middle module, A-GIS).

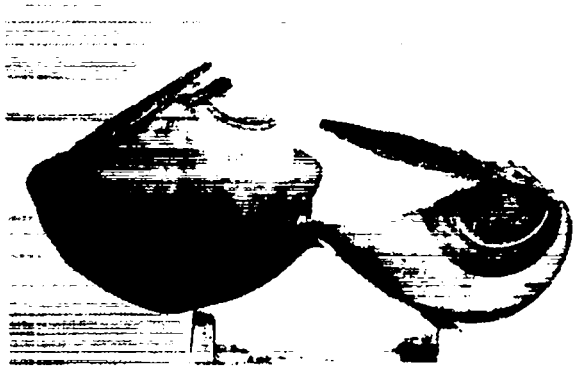

(b) (cont)

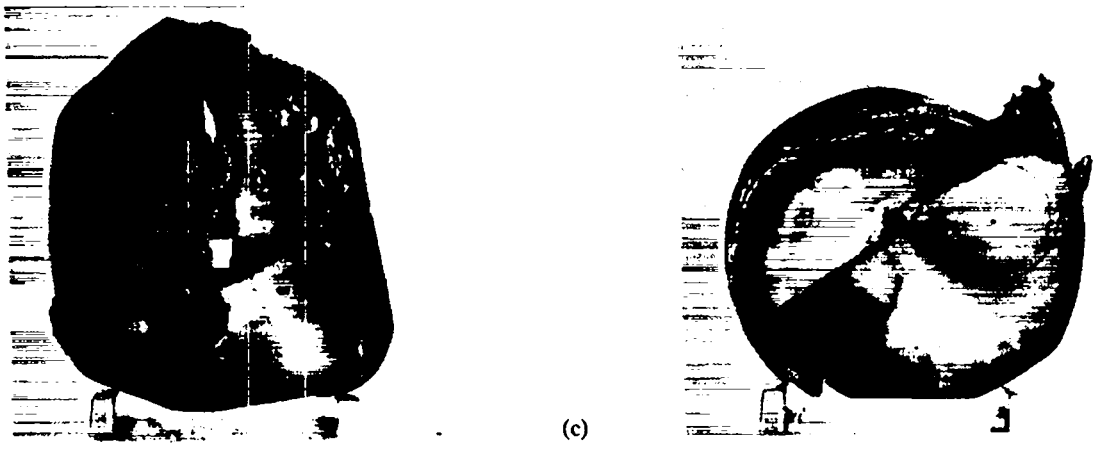

(c)

Fig. 53 (cont)

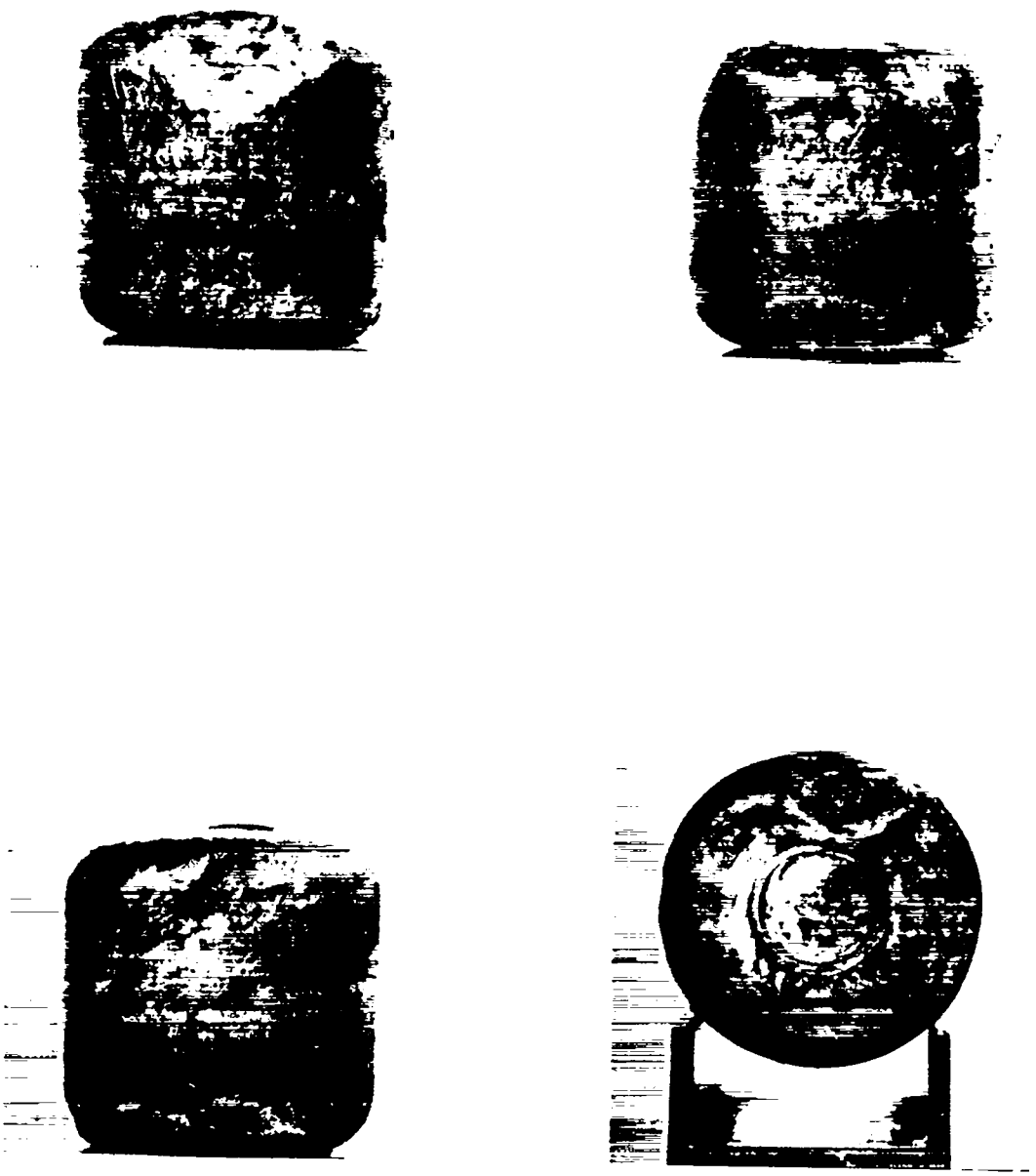

Fig. 54. Clad M-35 was recovered integral after CST-7-RTG-3 at 12.9 MPa.

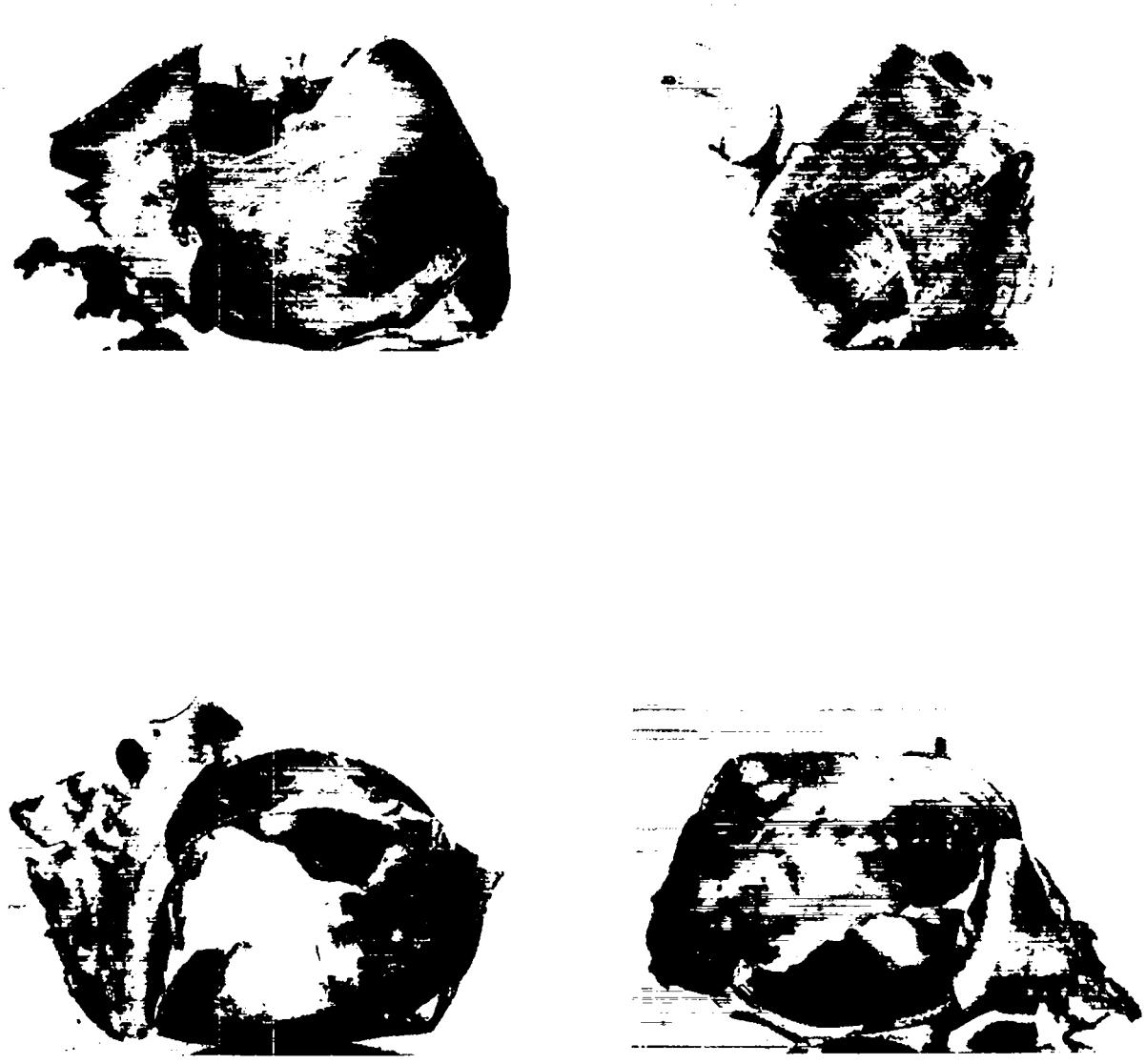

Fig. 55. Clad M-30 was breached in an overpressure test at 12.9 MPa by collision with either the shock tube or catch tube walls.

Fig. 56. Clad fragment from CST-7-RTG-3 recovered inside the catch tube; 40X.

Fig. 57. Fractured area on the surface of the clad fragment; electron micrograph, 2000X.

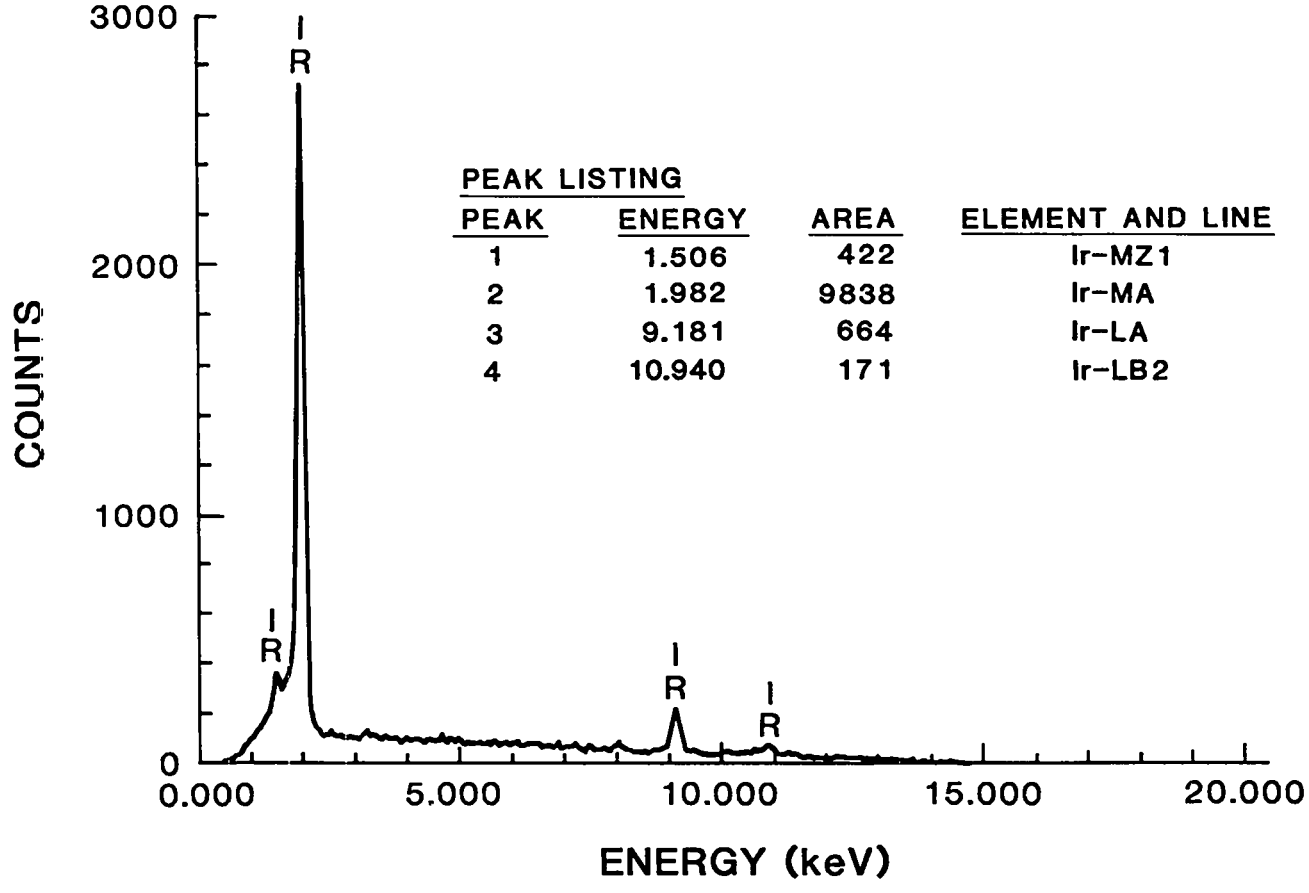

Fig. 58. X-ray spectrum from the area seen in Fig. 57 (50-s counting time). Only iridium was detected.

(a)

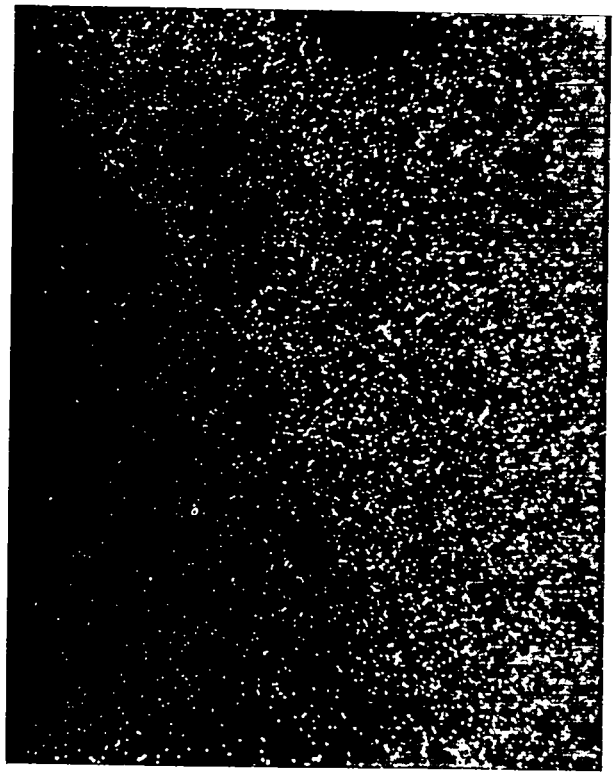

(b)

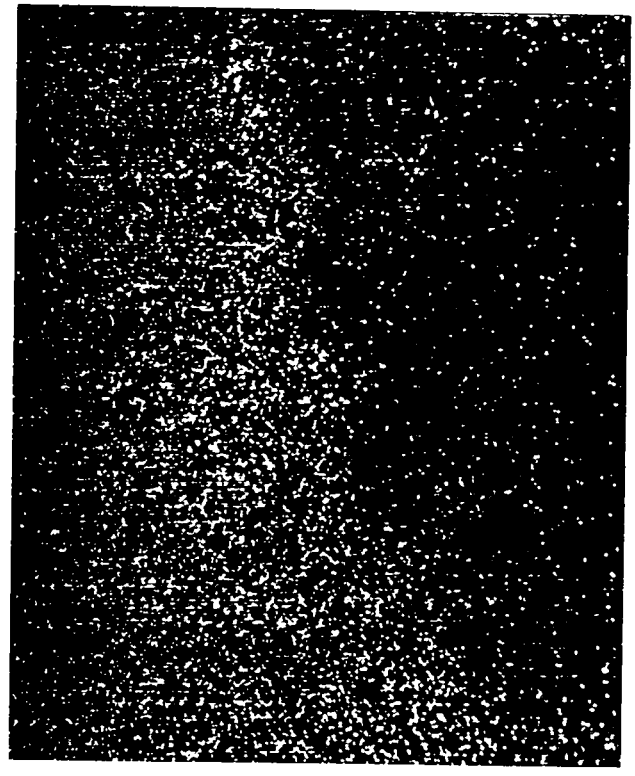

(c)

Fig. 59. Gouged area on the surface of the clad fragment: (a) Electron micrograph, (b) iron dot map, and (c) iridium dot map; all at 10000X.

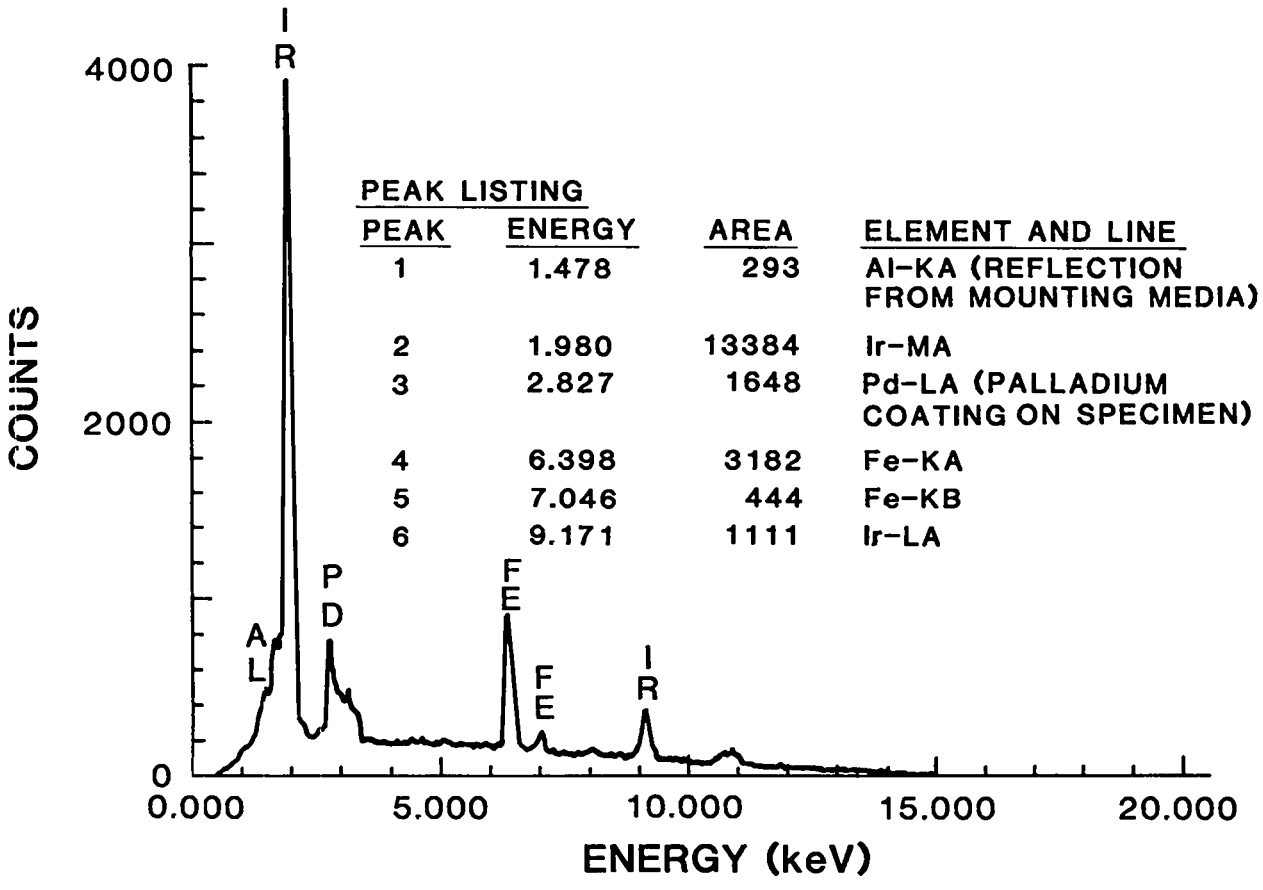

Fig. 60. X-ray spectrum from the area seen in Fig. 59 (262-s counting time). Both iridium and iron were detected.

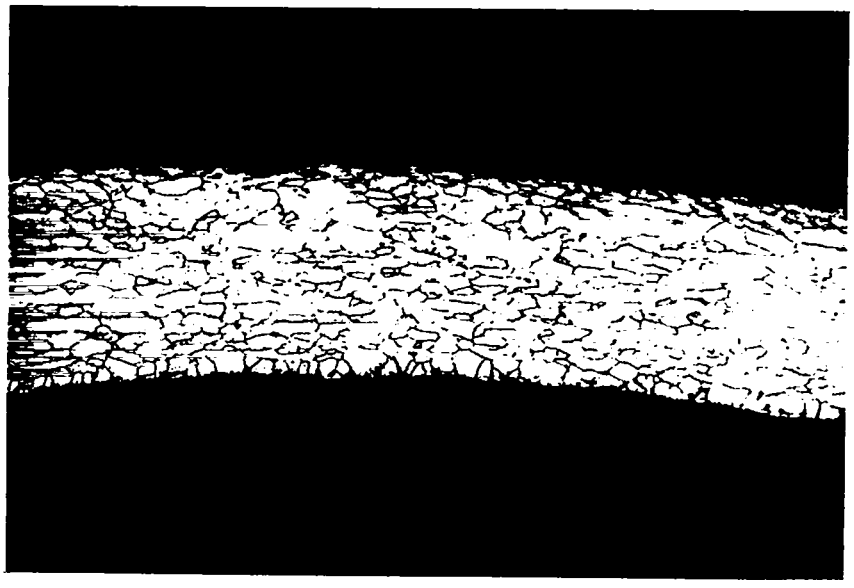

Fig. 61. Grain elongation and a reduction in thickness of 27% occurred in a section of the M-35 vent cup; 50X.

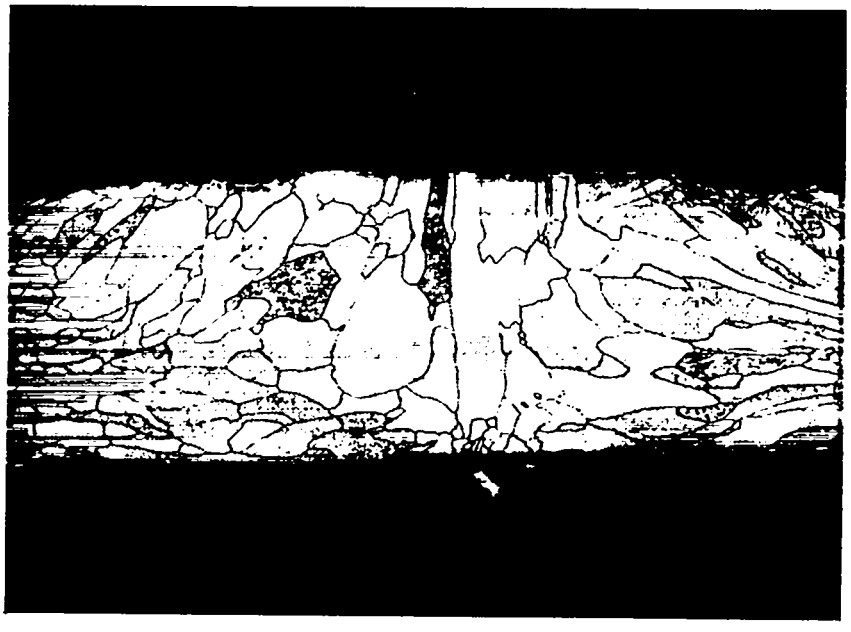

Fig. 62. The M-35 capsule weld was unusually coarse grained; 50X.

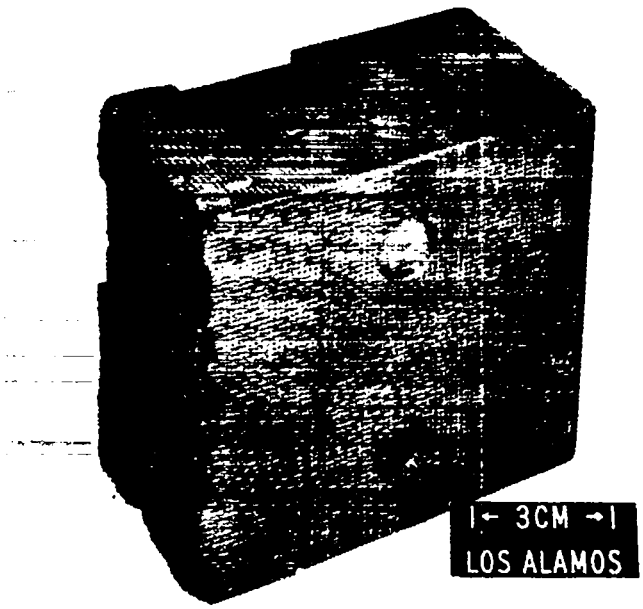

Fig. 63. The module exposed to an overpressure test at 2.96 MPa had a crack on each side of the broad faces of the aeroshell.

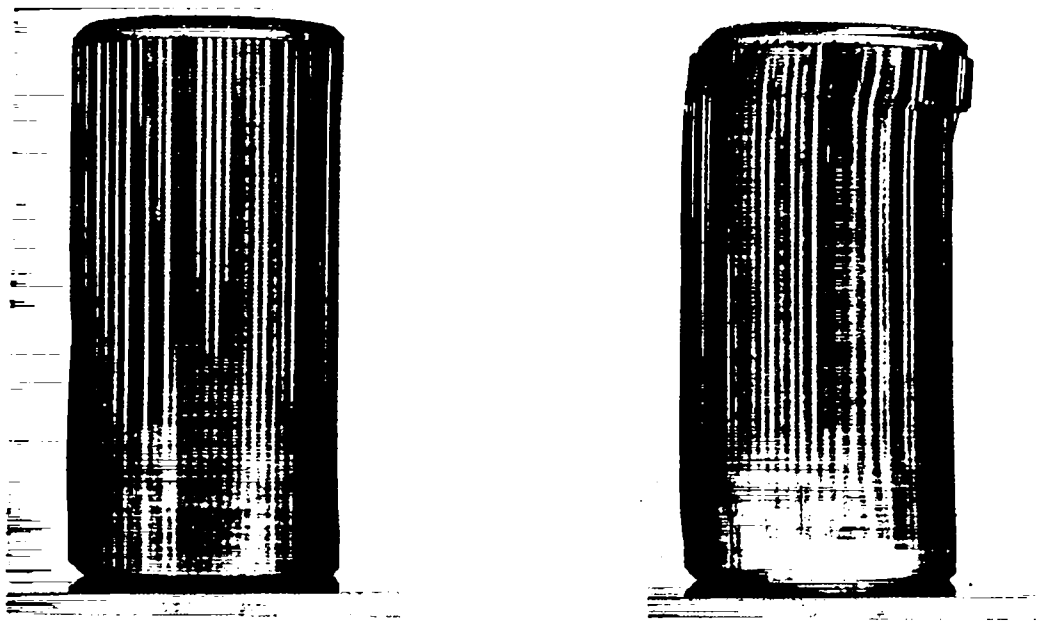

(a) (b)

Fig. 64. The A-GIS (a) and the C-GIS (b) from CST-8-RTG-4 were cracked.

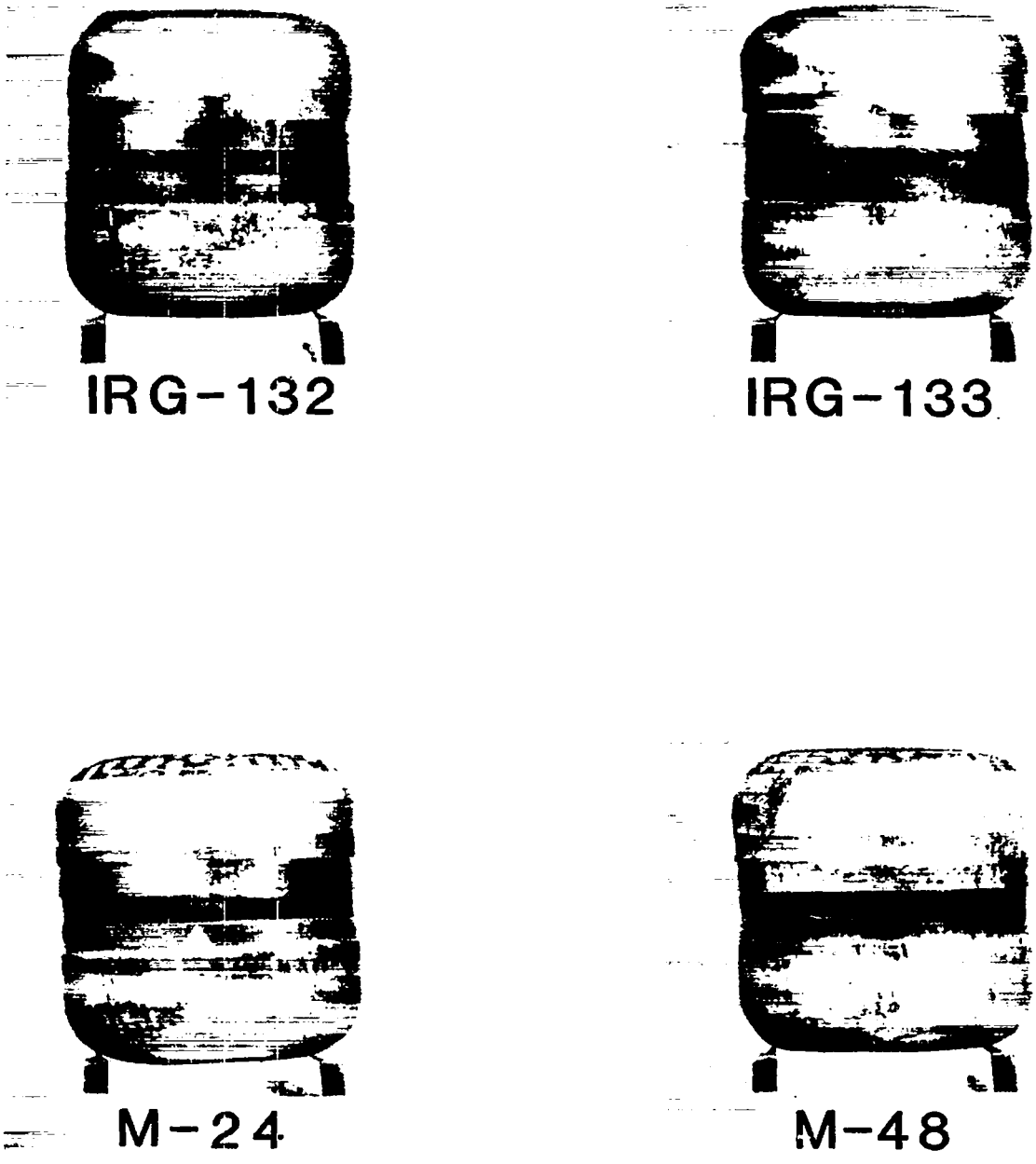

Fig. 65. The simulant-fueled clads exposed to 2.96 MPa were only slightly deformed.

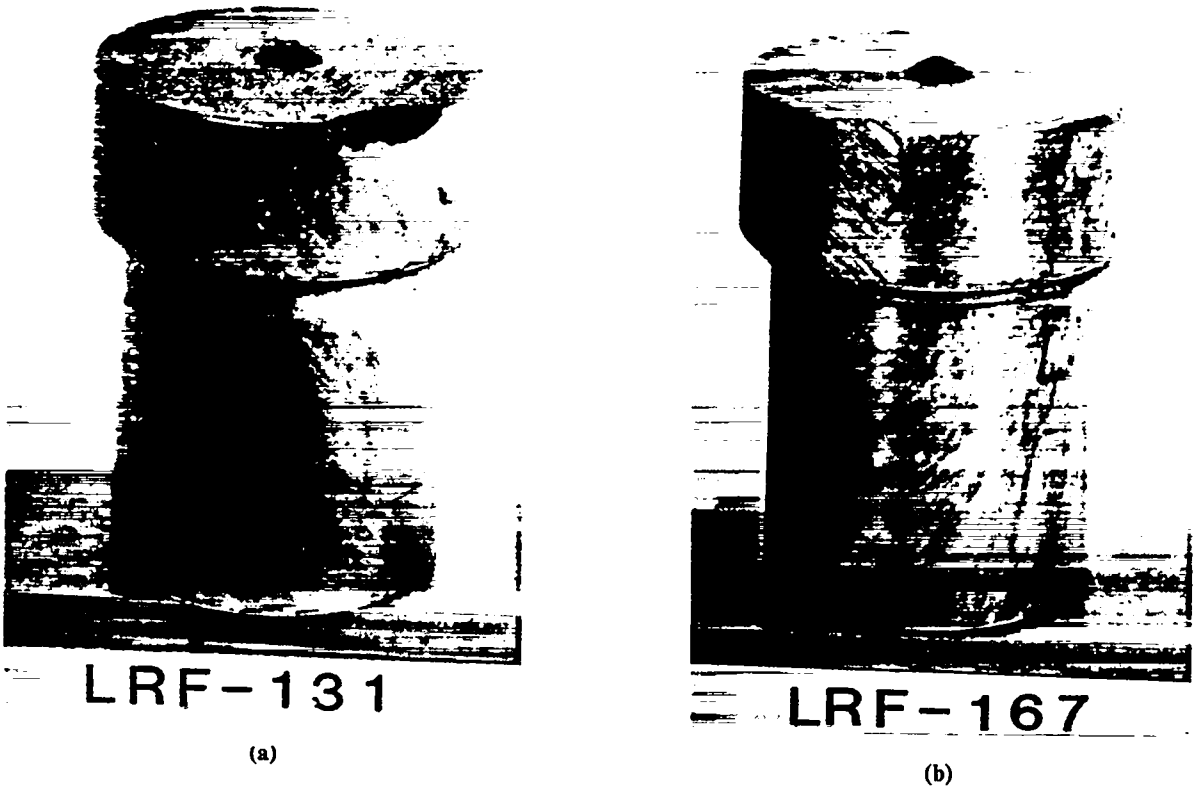

Fig. 66. The simulant-fueled LWRHUs were not significantly deformed after an explosion test at 2.96 MPa.

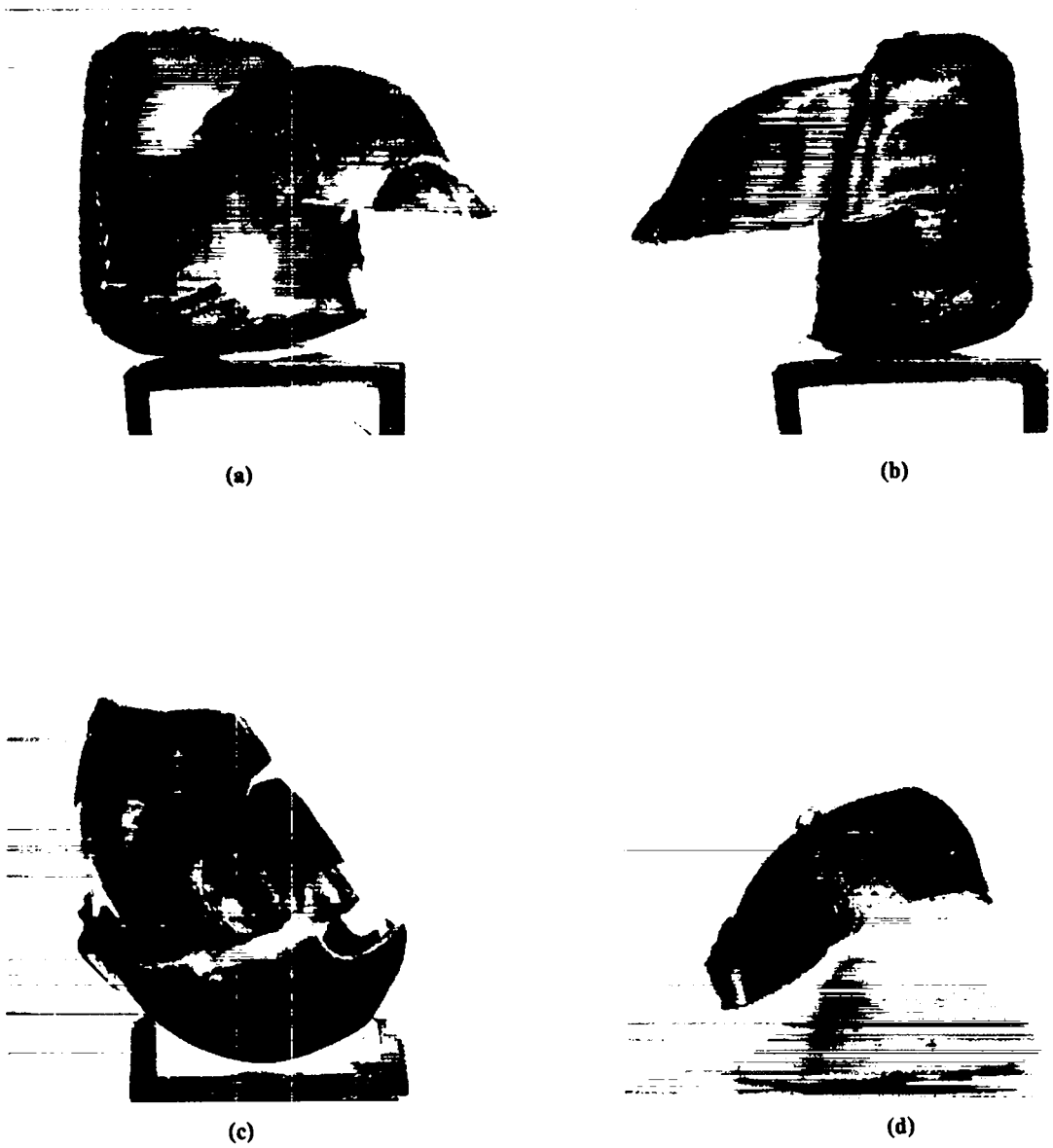

Fig. 67. Clad M-46 was recovered in two pieces after CST-9-RTG-5. The breach was a result of collision with either the shock tube or catch tube walls. Four views (a, b, c, d).

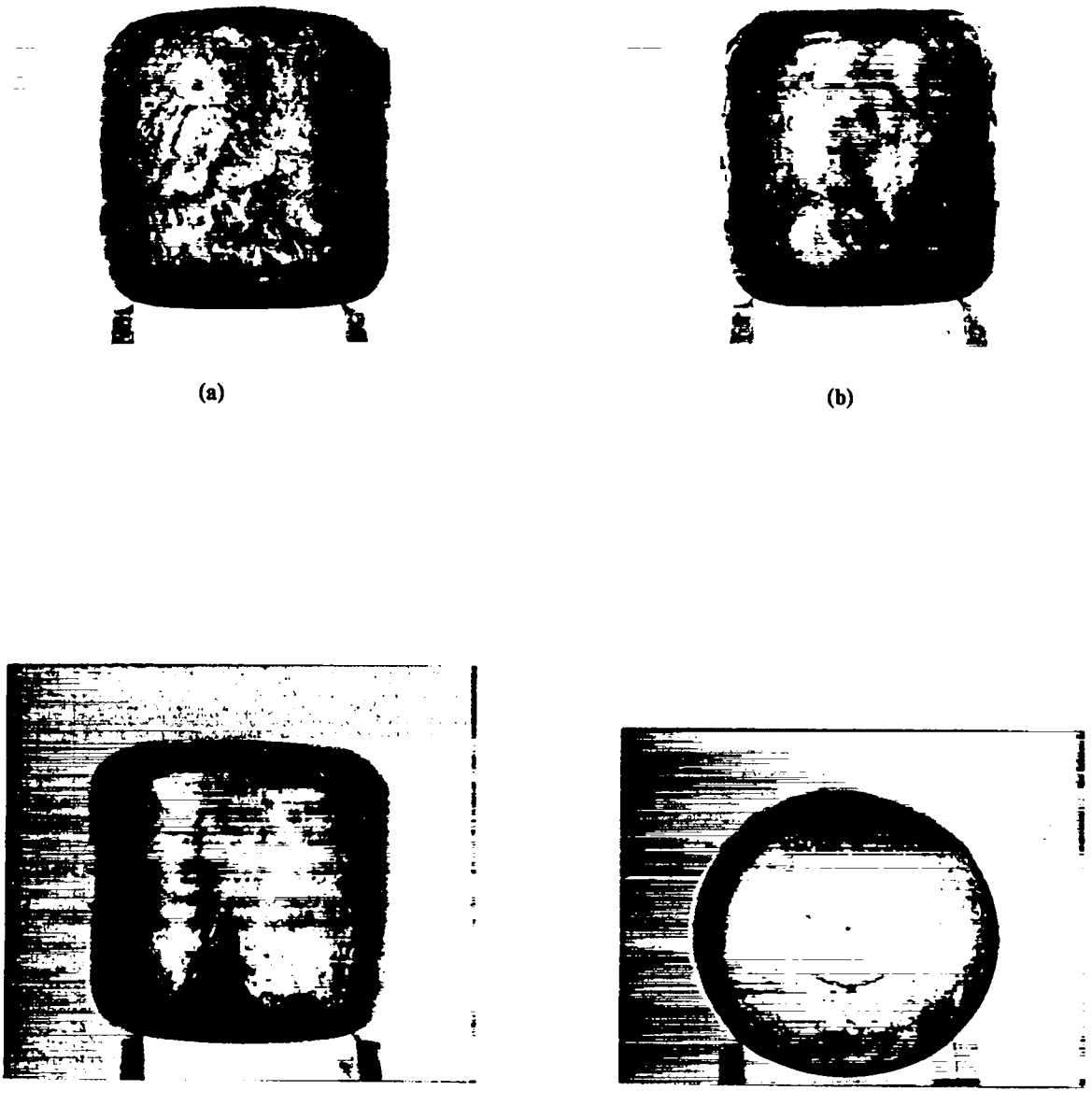

Fig. 68. Clad M-40 was recovered integral after exposure to 15.3 MPa in CST-9-RTG-5. Four views (a, b, c, d).

Fig. 69. An M-46 clad fragment containing striations and cracks on the external surface was selected for SEM examination; 7X.

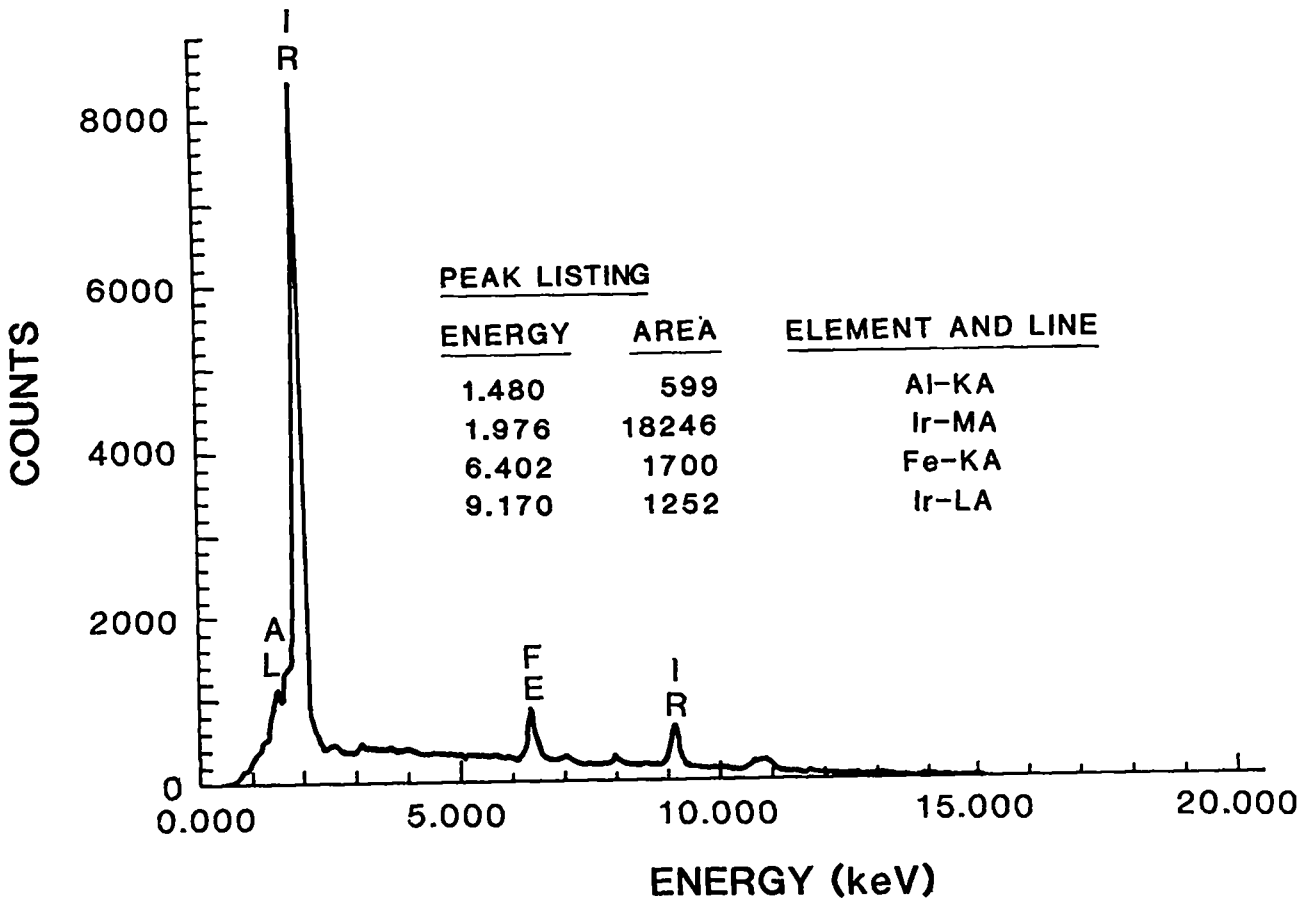

Fig. 70. Low-magnification x-ray spectra of the area in Fig. 71a (20-s counting time). Iridium, iron, and aluminum were detected.

(a)

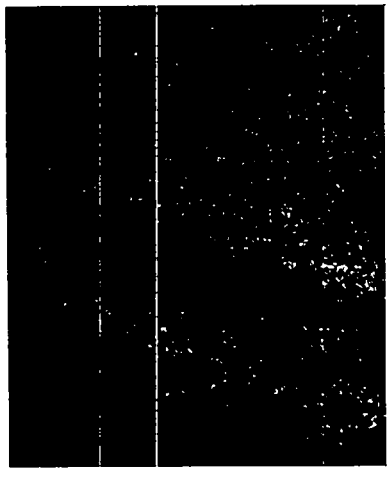

(b)

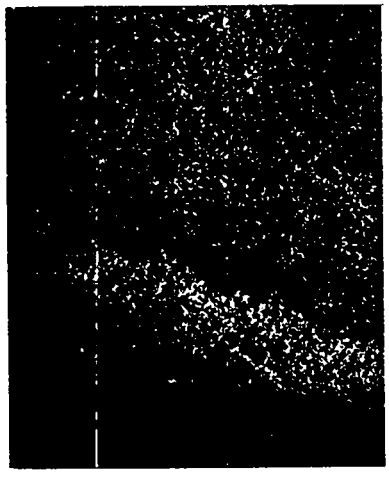

(c)

Fig. 71. M-46 fragment fracture surface: (a) Electron micrograph, (b) iridium dot map, and (c) iron dot map; all at 30X.

Note:
Figures (b) and (c) are reversed.

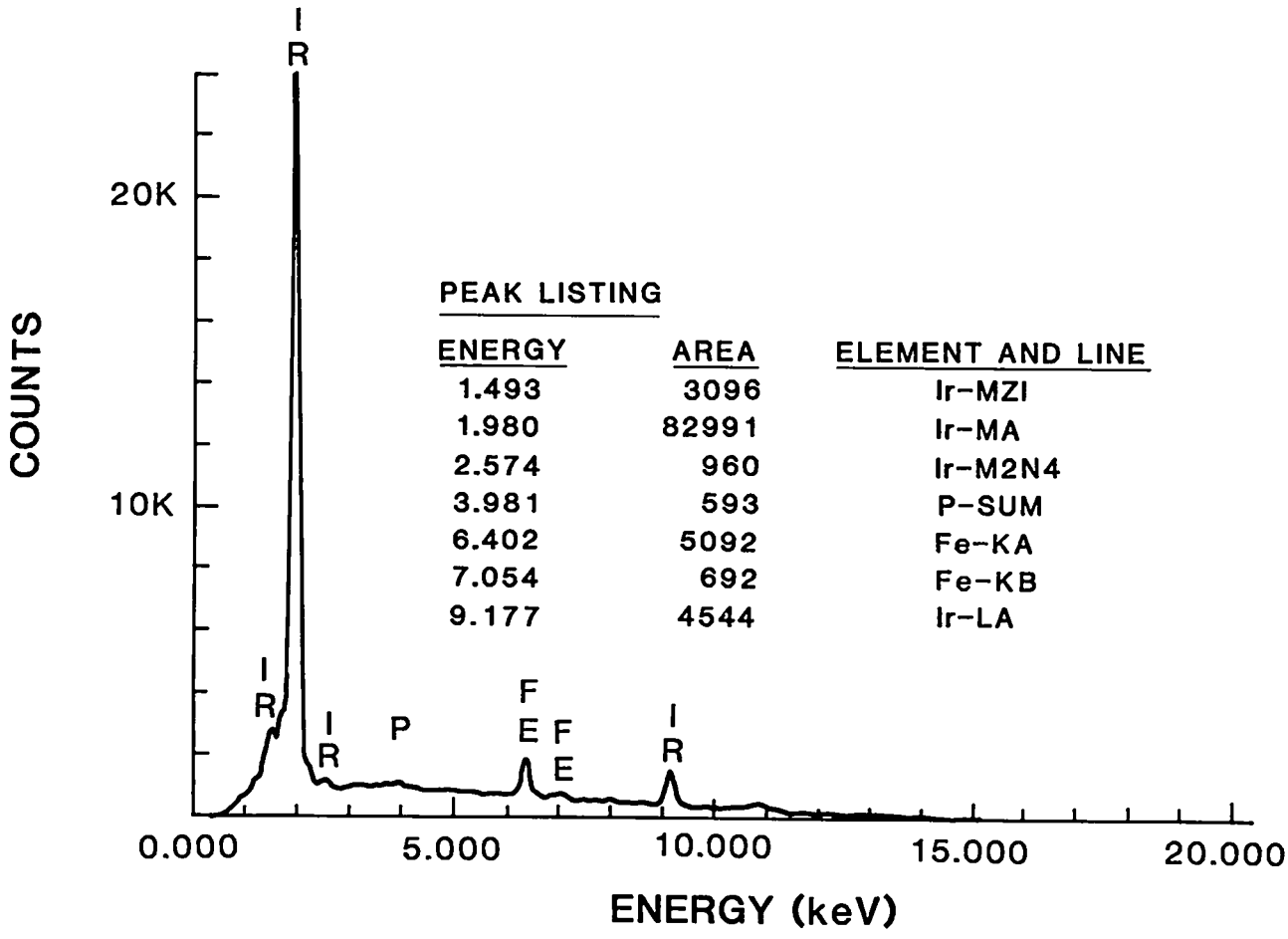

Fig. 72. X-ray spectra from the area in Fig. 73a (30-s counting time). Iridium, iron, and phosphorus were detected.

(a)

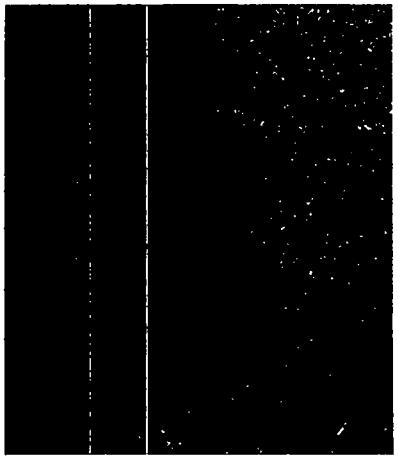

(b)

(c)

Fig. 73. Gouged area on surface of clad fragment: (a) Electron micrograph, (b) iridium dot map, and (c) iron dot map; all at 1000X.

Note:

Figures (b) and (c) are reversed.

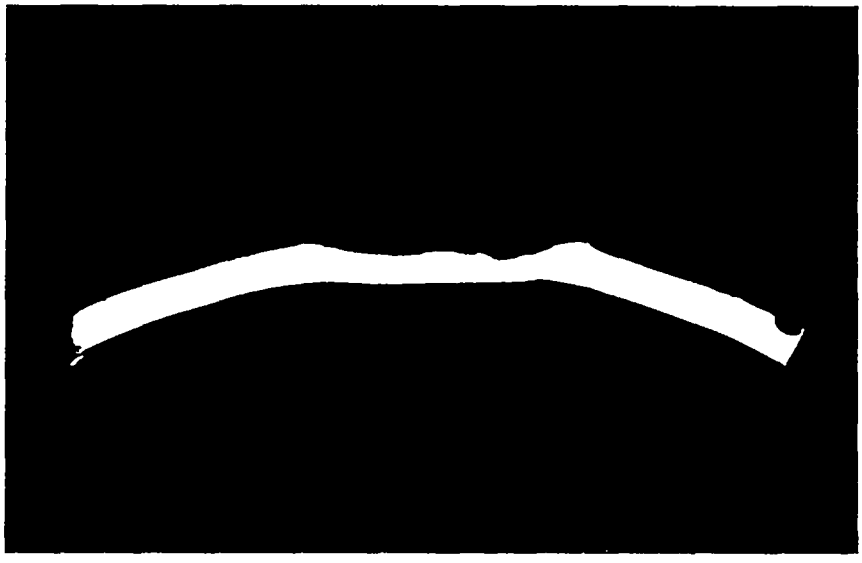

Fig. 74. A crater in the M-40 vent cup penetrated approximately 35% of the capsule wall; 6X.

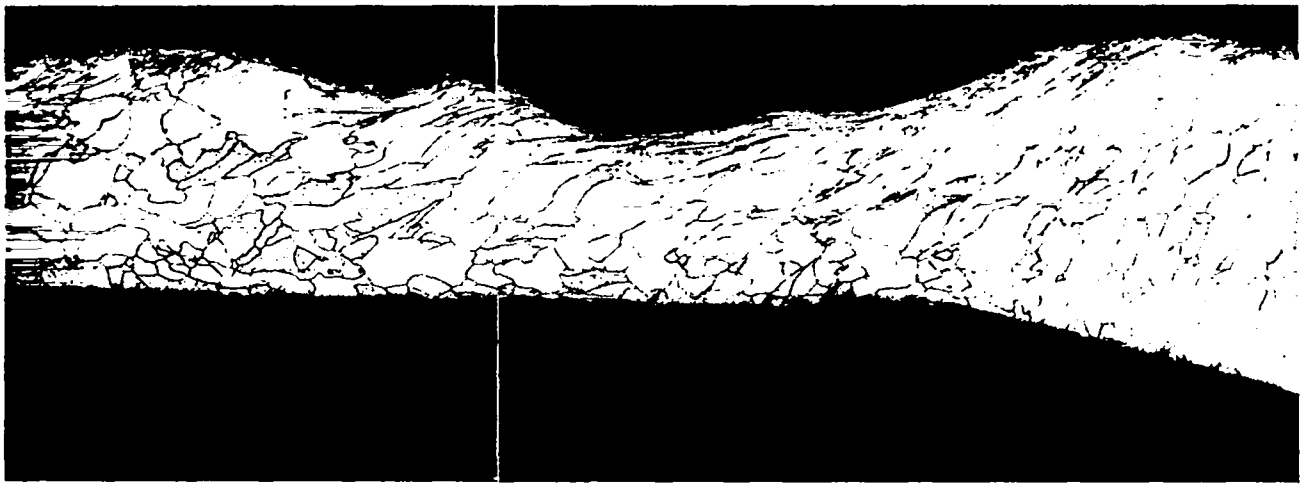

Fig. 75. Significant grain elongation occurred in the crater of the M-40 vent cup; 50X.

Printed in the United States of America
Available from
National Technical Information Service
US Department of Commerce
5285 Port Royal Road
Springfield, VA 22161
Microfiche (A01)

Page Range	NTIS Price Code	Page Range	NTIS Price Code	Page Range	NTIS Price Code	Page Range	NTIS Price Code
001-025	A02	151-175	A08	301-325	A14	451-475	A20
026-050	A03	176-200	A09	326-350	A15	476-500	A21
051-075	A04	201-225	A10	351-375	A16	501-525	A22
076-100	A05	226-250	A11	376-400	A17	526-550	A23
101-125	A06	251-275	A12	401-425	A18	551-575	A24
126-150	A07	276-300	A13	426-450	A19	576-600	A25
						601 up*	A99

*Contact NTIS for a price quote.

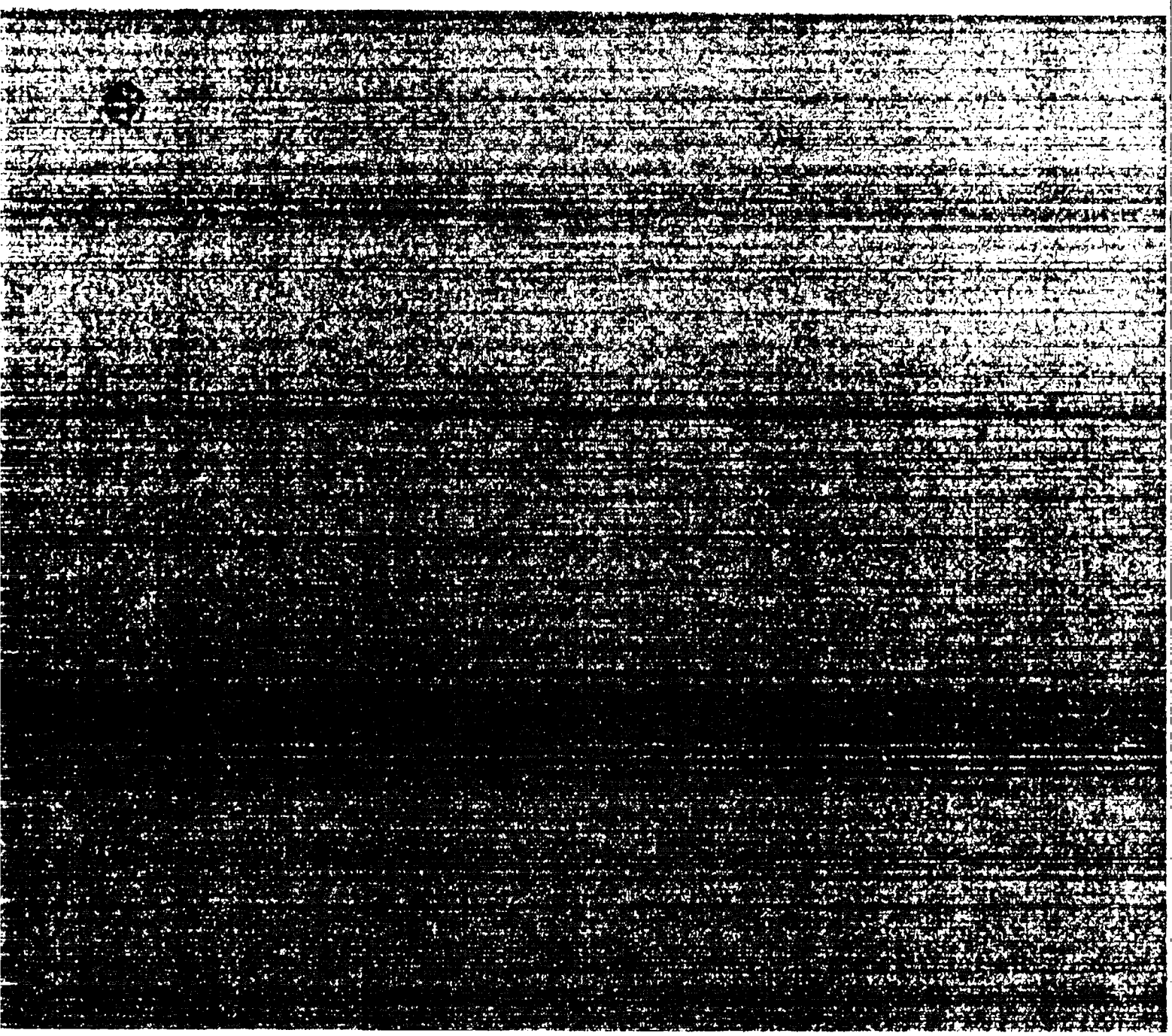

Los Alamos